




REVIEW ARTICLE

Simulating the blood-brain barrier by using artificial membranes, multicellular culturing systems, and high-tech applications

Hamdam Hourfar^{1*}, Arghavan Fattahi¹, Mohammad Raeji¹,
Kimia Marzookian¹, Naser Safari¹, Narges Nasrollahi Boroujeni¹,
Farhang Aliakbari¹, Daniel E. Otzen², Michael J. Strong^{3,4,5},
and Dina Morshedi^{1*}

¹Department of Bioprocess Engineering, National Institute of Genetic Engineering and Biotechnology, Tehran, Iran

²Department of Molecular Biology and Genetics, Interdisciplinary Nanoscience Centre (iNANO), Aarhus University, Aarhus C, Denmark

³Molecular Medicine Group, Robarts Research Institute, Schulich School of Medicine and Dentistry, Western University, London, Ontario, Canada

⁴Department of Clinical Neurological Sciences, Clinical Neurological Sciences, Schulich School of Medicine and Dentistry, Western University, London, Ontario, Canada

⁵Department of Pathology and Laboratory Medicine, Schulich School of Medicine and Dentistry, Western University, London, Ontario, Canada

(This article belongs to the *Special Issue: Biomedicine and Bioinformatics Engineering*)

*Corresponding authors:

Dina Morshedi
(morshedi@nigeb.ac.ir)
Hamdam Hourfar
(h_hourfar@nigeb.ac.ir)

Citation: Hourfar H, Fattahi A, Raeji M, *et al.* Simulating the blood-brain barrier by using artificial membranes, multicellular culturing systems, and high-tech applications. *J Clin Transl Res.* 2026;12(2):025390064.
doi: 10.36922/JCTR025390064

Received: September 23, 2025

Revised: November 16, 2025

Accepted: December 4, 2025

Published online: February 19, 2026

Copyright: 2026 Author(s).

This is an open-access article distributed under the terms of the Creative Commons AttributionNon-Commercial 4.0 International (CC BY-NC 4.0), which permits all non-commercial use, distribution, and reproduction in any medium, provided the original work is properly cited.

Publisher's Note: AccScience Publishing remains neutral with regard to jurisdictional claims in published maps and institutional affiliations.

Abstract

Background: The blood-brain barrier (BBB) is an intricate structure of the vascular endothelium that regulates trafficking required for cerebral homeostasis via tightly regulated influx and efflux transport mechanisms. It also performs a critical function in mediating communication between the periphery and the central nervous system (CNS). The BBB is designed to maintain a precisely regulated microenvironment conducive to normal neuronal activity. The development of *in vitro* BBB models has been driven by the need for a fast, reliable, and cost-effective tool to study the complexities of the BBB and to screen potential CNS drugs. **Aim:** This review provides readers with a concise yet comprehensive introduction to the fundamental histology of the BBB. This background is essential for interpreting model design constraints and limitations in BBB simulation. Following that, we thoroughly examine *in vitro* models, providing a comprehensive analysis of their applications and the equations used to assess specific BBB parameters. **Relevance for patients:** From a translational and clinical perspective, *in vitro* models of the BBB have the potential to provide novel insights into brain pathophysiology under adverse conditions, including brain tumors, traumatic injuries, strokes, and neurodegenerative disorders, and ultimately aid in the discovery of effective treatment strategies.

Keywords: Blood-brain barrier; *In vitro* blood-brain barrier models; Integrity assays; Neurovascular unit

1. Introduction

The cerebral blood-brain barrier (BBB) is a complex interface between the central nervous system (CNS) and the peripheral blood circulation, with vital protective and regulatory functions. This barrier possesses an exceptional ability to control the transfer of substances and immune cells between the blood and the brain. The properties of the BBB mainly refer to the unique characteristics of its constituent endothelial cells (ECs) and their interactions with other neural cells, known as the neurovascular unit (NVU), which exhibit different behaviors under different conditions.¹ In 1695, Ridley² was the first to describe the limited permeability of brain blood vessels; this historical point has been reviewed by Liddelow.³ Ehrlich⁴ subsequently confirmed the physiological protective function of the BBB by injecting dye into the circulatory system of rats; this experiment is summarized in Barichello *et al.*,⁵ who attributed the dye's limited penetration to its low affinity for the CNS. On the other hand, Goldman⁶ injected a similar dye into the subarachnoid space, resulting in staining of the CNS while peripheral tissues remained unstained. Later, using electron microscopy, Reese and Karnovsky⁷ demonstrated that the tight junctions (TJs) between capillary ECs that form the BBB confer its impenetrability. More recent research has revealed further details about the BBB's distinctiveness.

The BBB poses a major barrier to the delivery of therapeutics to the brain. A key challenge is translating findings from experimental models in the laboratory to models tested in live animals and, eventually, to human clinical trials. Consequently, there is an increasing demand for the development of more robust BBB models to enhance neuroscience research across different areas.⁸ After providing a brief overview of human BBB structure and characteristics, this review extensively explores and assesses current *in vitro* models of the BBB, both static and dynamic, which incorporate cells or cell-free techniques. In addition, we describe recent breakthroughs and outline prospective future developments in this rapidly evolving field.

In addition, we provide a comprehensive overview of BBB models ranging from simple to advanced systems, and we summarize methods for validating cell-based BBB models, together with an updated description of BBB structure and key characteristics, to improve understanding of BBB dynamics and support CNS drug discovery.

2. Characteristics of the BBB structure

The brain is a uniquely regulated organ whose microenvironment is maintained by specialized barrier systems, including the BBB. The BBB constitutes a highly

restrictive barrier in the brain vascular (BV) system that strongly restricts the entry and exit of materials, with low paracellular permeability and low transcytosis.^{9,10} Gaining a comprehensive understanding of the BBB constituents holds great potential for enhancing neurological models and optimizing the design of novel strategies to improve the delivery of therapeutic drugs. Figure 1 shows a general diagram of the brain's blood vessels and its constituent, the NVU, along with details of the components that make up the NVU.

2.1. Endothelial TJs

The BBB is formed by closely connected brain microvessel ECs (BMECs). These cells, by forming constricted junctions with each other, create a compact structure that plays a vital role in the proper function of the BBB (Figure 1).¹¹ There are three types of junction complexes between BMECs that contribute to the structure and function of the BBB. These junctional connections include TJs, adherens junctions (AJs), and gap junctions. In the following sections, each of these types is discussed in detail, and their characteristics are summarized in Table 1.¹¹ Junctional connections can be found in the brain and peripheral tissues, such as the intestine, stomach, liver, and pancreas. However, endothelial TJs in the brain are more resistant to substances than are the corresponding TJs in other tissues. In addition, cytoplasmic scaffolding proteins, such as Zonula occludens (ZO) and the actin cytoskeleton, accompanied by TJs, are involved in intercellular interactions.¹² ZO proteins (ZO-1, ZO-2, ZO-3) are membrane-associated cytoplasmic proteins in the BBB that, through the first PDZ domain, interact directly with the C-terminal domain of claudins and attach transmembrane proteins to the actin cytoskeleton in EC membranes.¹³ In addition, TJs are involved in various cellular functions; for example, they participate in cellular communication and control the transport of ions and tissue equilibrium.¹¹ In addition, they are involved in regulating cellular signaling pathways, such as cell proliferation, differentiation, and migration. In addition, dysfunction of these proteins disrupts apoptotic signaling and alters levels of inflammatory cytokines, which can lead to various diseases, including multiple sclerosis, inflammatory bowel disease, and even cancers.¹⁴

2.2. The development of the NVU relies on certain considerations of cellular members and signaling pathways

The unique features of brain ECs are attributed to specific characteristics of their lipid composition in addition to their close connections through specific junctions. In addition, these properties are closely associated with other components of the NVU. The NVU is a complex cellular

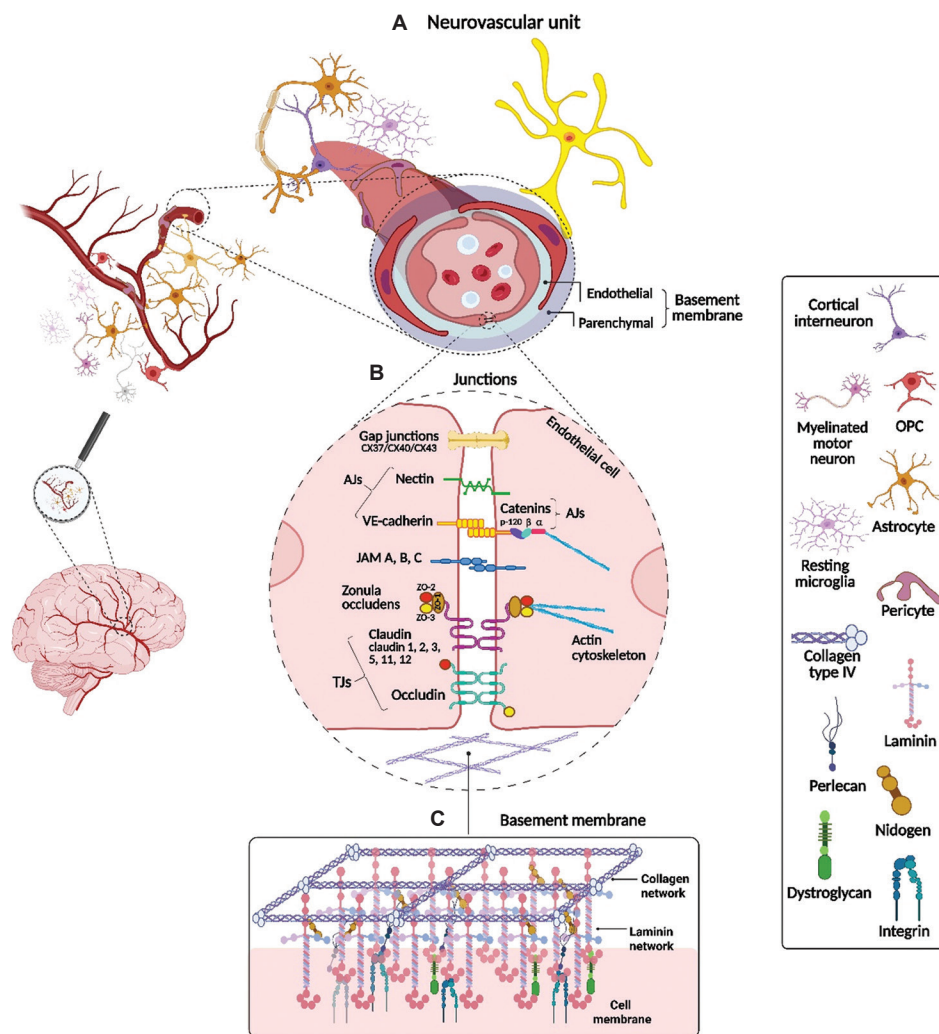


Figure 1. Blood-brain barrier junctional proteins and basement membrane proteins, along with neurovascular unit (NVU) cells. (A) The cellular components of the NVU consist of endothelial cells, astrocytes, pericytes, neurons, and microglia. (B) Tight junctions, adherens junctions, gap junctions, and junctional adherens molecules lining the endothelial cell interface, preventing transportation of molecules via the paracellular pathway. (C) The basement membrane between the endothelial layer and astrocytes consists of collagen IV and laminin networks, connected to each other and to membrane receptors (integrins and dystroglycans), through proteoglycans, such as nidogen and perlecan. Created in BioRender. Aliakbari, F. (2026) <https://BioRender.com/xfle8ty>.

system that includes neurons, astrocytes, microglia, oligodendrocytes, smooth muscle cells, and pericytes covering the basal lamina, ECs, extracellular matrix (ECM), and circulating blood components.^{29,30}

Growth factors released during neural tube development significantly influence the formation of the BBB and its distinct characteristics. Specifically, vascular endothelial growth factor (VEGF)^{31,32} and signaling pathways, such as the Wnt/ β -catenin and Sonic Hedgehog pathways, play crucial roles in the development of the BBB by controlling and balancing different aspects of BBB maintenance along with specialized angiogenesis (growth of new blood vessels).³³⁻³⁵

In addition, the basement membrane (BM) and glycocalyx, non-cellular constituents of the NVU located in proximity to the endothelial layer, also contribute to the unique features of the BBB.³⁶ Both are discussed in the following sections.

2.3. Role of glycocalyx

The glycocalyx, a gel-like negatively charged layer, is primarily composed of cell-bound proteoglycan core proteins, glycosaminoglycan side chains, and hyaluronan.³⁷ The endothelial glycocalyx is denser in the cerebral vasculature than in the cardiovascular and pulmonary capillaries.³⁸ The different components of the endothelial glycocalyx are schematized in Figure 2.

Table 1. The different kinds of junctional proteins present in the BBB

Group	Protein type	Functions	References
Transmembraneproteins			
TJs	Claudin (claudin-1, claudin-2, claudin-3, claudin-5, claudin-11, claudin-12)	Forms the paracellular ion pore Determines paracellular tightness	15
	Occludin	Regulates adhesion between ECs Helps to organize the claudin-5 strand	15,16
	Tricellulin (marvelD2)	Involved in tricellular and bicellular contacts Limits blood to brain movement of large molecules via the paracellular route	17,18
	JAM (JAM-A, JAM-B, JAM-C)	Participates in the formation of tight junctions and the determination of paracellular permeability Role in the transmigration of leukocytes	19
	MarvelD3	Exact function unknown, but presumed to determine epithelial paracellular permeability and increase TEER. Not required for the formation of the BBB	20,21
AJs	Cadherin (vascular endothelial-cadherin, epithelial-cadherin, neural-cadherin)	Adhesion between cells and cytoplasmic/scaffolding proteins Contributes to endothelial survival, blood vessel assembly, and stabilization of the BBB	11,22,23
	Catenin (α -catenin, β -catenin, p120-catenin, plakoglobin)	Supports cadherin association and maintenance of TJ Regulates out-in signaling processes Controls endothelial barrier permeability	11,23,24
	Nectin	Formation of TJs and AJs through connections with the actin cytoskeleton	25
GJs	Cx (Cx37, Cx40, Cx43)	Regulatory role in cell proliferation, differentiation, and migration Communication between ECs Provides metabolic, electrical, and solute and molecule exchange coupling between cells Growth, development, and tissue homeostasis	11,14,26,27
Scaffolding protein			
ZO	ZO proteins (ZO-1, ZO-2, ZO-3)	Anchors transmembrane proteins to the actin cytoskeleton Essential for transmembrane and immunoglobulin protein assembly in the TJ of the BBB	28

Abbreviations: AJs: Adherens junctions; BBB: Blood-brain barrier; Cx: Connexin; GJs: Gap junctions; JAM: Junctional adhesion molecule; TEER: Transepithelial/transendothelial electrical resistance; TJs: Tight junctions; ZO: Zonula occludens.

The endothelial glycocalyx is considered one of the elements controlling BBB permeability.³⁹ It protects the vessel wall against circulating cells, prevents the passage of molecules larger than 70 kDa, and maintains homeostasis.⁴⁰ Increased histone deacetylase expression is commonly associated with the upregulation of matrix metalloproteinases (MMPs), heparinase, and hyaluronidase. The overexpression of these enzymes degrades the endothelial glycocalyx, leading to various destructive effects, including vascular hyperpermeability, inflammation, and coagulation, due to enhanced adhesion of ECs to blood cells.⁴¹

The glycocalyx coats the luminal surface of ECs and is in direct contact with flowing blood. Simultaneously, the BM is a thin layer situated below the ECs, extending into the brain's internal regions.⁴⁰

2.4. BM

The BV-BM helps preserve the integrity of the BBB, facilitates cell adhesion, regulates morphogenesis, promotes tubular monolayer formation, and supports cell proliferation, migration, and differentiation. This section provides a brief overview of the composition, structure, and physiological functions of the vascular BM. In addition, we discuss the potential of utilizing BM as a biomimetic material to develop high-quality *in vitro* BBB models.

The BM forms a thin, sheet-like layer on the basolateral side of ECs, separating them from the adjacent connective tissues. Two BMs surround brain microvessels: Endothelial BM (secreted by ECs) and parenchymal BM (secreted by astrocytes). The pericytes that are embedded between the two BMs also produce BM components. The four major

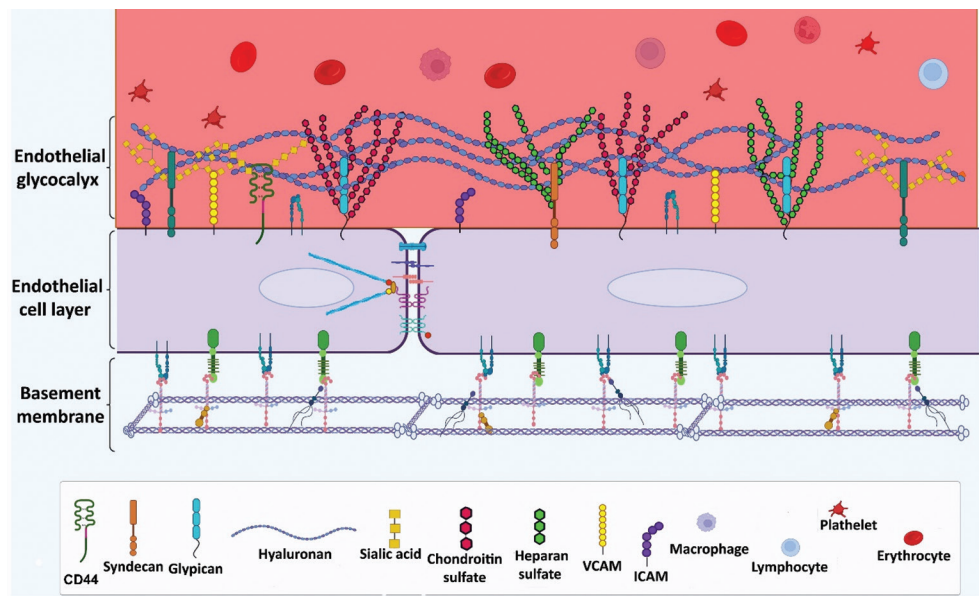


Figure 2. Schematic presentation of the relationship between the glycocalyx, basement membrane, and the brain's endothelial cells. Created in BioRender. Aliakbari, F. (2026) <https://BioRender.com/2qia9fw>. Abbreviations: CD: Cluster of differentiation; ICAM: Intercellular adhesion molecule; VCAM: Vascular cell adhesion molecule.

Table 2. The main BM proteins and their relationship to brain disorders and BBB integrity

BM component	Contribution to BBB integrity	References
Laminin	<ul style="list-style-type: none">- Involved in BBB repair after hypoxic injury and inflammation- Attenuates BBB damage after ICH- Maintains BBB integrity by inhibiting pericyte differentiation- Astrocytic end-feet polarization, induction of TJs expression in ECs	29,49-51
Collagen type IV	<ul style="list-style-type: none">- Collagen α chains protect from ICH and stroke	52
Perlecan	<ul style="list-style-type: none">- Integrin binding-dependent regulation of the BBB- C-terminal domain shows post-stroke neuroprotective effects	53
Agrin	<ul style="list-style-type: none">- Stabilization of vascular endothelial-cadherin, β-catenin, and ZO-1 in BMECs- Agrin downregulation leads to a decrease in astrocyte polarity and BBB leakage in CCH	54
Nidogen	<ul style="list-style-type: none">- Collective loss of both nidogen-1 and nidogen-2 causes damaged BM and perinatal death in mice	55

Abbreviations: BBB: Blood-brain barrier; BM: Basement membrane; BMECs: Brain microvessel endothelial cells; CCH: Cerebral chronic hypo-perfusion; EC: Endothelial cell; ICH: Intracerebral hemorrhage; TJs: Tight junctions; ZO: Zonula occludens.

constituents of BV-BM are laminins, collagen type IV, heparan sulfate proteoglycans (HSPGs), and nidogen (entactin) (Figure 2). Other minor BM macromolecules include fibronectin, the cell-matrix-modulating protein, secreted protein acidic and rich in cysteine (SPARC), also known as osteonectin.⁴²

A summary of the main functions of BV-BM components within the NVU is provided in Table 2. Among BV-BM proteins, laminins were the first principal component identified.⁴³ They are a family of heterotrimeric glycoproteins (with α , β , and γ chains) containing 16 isoforms.⁴⁴ BV ECs and pericytes produce laminin-411 and 511 (with $\alpha 4$ and $\alpha 5$ chains), and astrocytes mainly secrete laminin-211.^{45,46} The most abundant component of the

BM is collagen type IV, which has a non-fibrillar structure composed of three α chains. Collagen $\alpha 1(IV)2\alpha 2(IV)$ is the major isoform of collagen type IV in the vascular BM.^{47,48}

Among the minor non-structural constituents of BM, nidogens (nidogen-1 and nidogen-2) possess binding sites for the laminin and collagen IV isoforms and stabilize the BM.⁵⁶ HSPGs are also involved in the structural maintenance of BV-BM and the robustness of the BBB. Perlecan (HSPG-2) can interact with different growth factors, e.g., fibroblast growth factor (FGF) 2, VEGF, and platelet-derived growth factor.⁵⁷ Agrin, another notable BM proteoglycan, stabilizes BV-BM by binding to α -dystroglycan and laminin.⁵⁸ Another minor

non-structural constituent of BM is SPARC, a member of the matricellular protein family involved in angiogenesis.⁵⁹

3. The mechanisms of passage through the BBB

In the previous sections, we discussed how the BBB prevents the free movement of molecules between the blood and the brain. Here, we will briefly discuss the various ways in which molecules can be transported across the BBB. These categories include passive diffusion, ion transport, carrier-mediated transport through influx and efflux transporters, and specific receptor-mediated and adsorptive transcytosis mechanisms (Figure 3).¹⁰

Passive diffusion is a physicochemical process that relies on the structural characteristics of compounds.¹⁰ Several essential parameters, particularly lipophilicity, molecular weight (MW), hydrogen bonding (HB) index, polar surface area (PSA), and cross-sectional area (CSA), are crucial for determining the potential for passive diffusion across the BBB. Lipophilicity can be assessed by the LogP parameter, which indicates the compound's preference for lipid-based environments compared to an aqueous environment.⁶⁰

Unsurprisingly, small molecules with MWs below 400 Da more easily undergo passive diffusion and transport through the BBB than larger molecules. However, the ability of a compound to undergo passive diffusion is

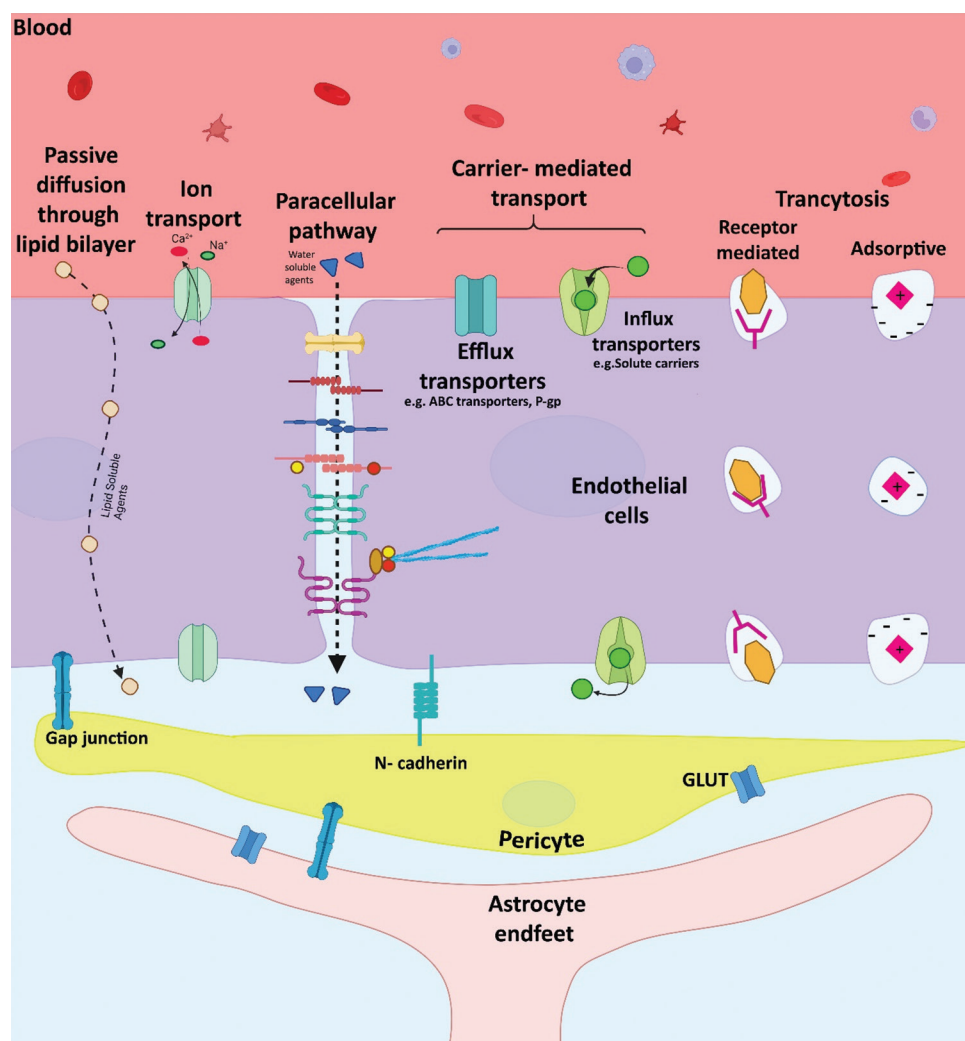


Figure 3. Schematic overview of blood–brain barrier (BBB) transport mechanisms. Water-soluble and lipid-soluble agents, as well as small ions, can cross the BBB via paracellular routes, passive diffusion through the lipid bilayer, and ion transport mechanisms, respectively. Carrier-mediated transport (e.g., influx and efflux transporters) and receptor-mediated or adsorptive transcytosis mediate the transfer of selected molecules between blood and brain. Created in BioRender. Aliakbari, F. (2026) <https://BioRender.com/bqg3r5n>. Abbreviations: GLUT: Glucose transporter; P-gps: P-glycoprotein.

also influenced by other factors.⁶¹ Thus, an increase in the HB index (HB capabilities) tends to decrease the rate of passive diffusion.^{62,63} Similarly, an increase in PSA (i.e., the contribution of polar atoms, such as nitrogen and oxygen, to the surface area) reduces passive diffusion.⁶⁴ Both the HB index and PSA reflect the amount of desolvation (removal of water molecules) accompanying membrane transport; the greater this amount is, the more difficult it is for the compound to traverse the hydrophobic part of the membrane. The orientation of a ligand in the membrane can also have a significant effect on BBB penetration. The CSA measures the area occupied by a compound in the lipid membrane. CSA considers the flexibility of a molecule and its impact on permeation.⁶⁵ The molecular volume is another factor that is related to a molecule's MW and structure. It accounts for all accessible conformations the molecule can adopt under physiological conditions and is related to the number of rotatable bonds and rings in the molecule.⁶⁶

Carrier-mediated transport utilizes specific influx and efflux transporters to facilitate the transport of materials across the BBB. In addition, specific receptor-mediated and adsorptive transcytosis are mechanisms by which the BBB allows the passage of certain substances. For instance, nutrients such as folates and amino acids, as well as molecular carriers such as transferrin, can permeate the BBB through receptor-mediated transport mechanisms. This process involves vesicular endocytosis, during which molecules are taken up into vesicles within BBB cells. Various *in vitro* BBB models have been developed and widely utilized to better understand and evaluate the transport properties of molecules across the BBB. These models enable assessment of transportation efficiency and evaluation of candidate delivery strategies.

In neurovascular research, whether for drug discovery or to investigate BBB alterations in neurological disorders, designing experimental models mimicking its complex physiology is a critical requirement for scientists. In this context, insights from exploring BBB characteristics and its transport properties could serve as a basis for designing BBB experimental models and selecting appropriate *in vitro* models to reproduce key structural and functional characteristics of the barrier, allowing more accessible, controllable, and cost-effective models. Accordingly, various *in vitro* BBB models have been developed and are discussed in the following sections.

4. *In vitro* BBB models

The development of *in vivo* and *in vitro* BBB models encounters numerous challenges that require careful consideration to ensure accuracy and relevance in studying

the BBB and creating efficient brain therapeutics. This is not a trivial task, as the BBB is an intricate structure in which all members of the NVU components interact to establish and maintain BBB function.

Species-specific differences in efflux transporters, TJs, and cell-cell signaling between laboratory animals and humans can lead to inaccurate conclusions in *in vivo* BBB models. In addition, the utilization of these models for drug discovery poses various challenges, such as the need for specialized equipment and reagents, careful observation, ethical considerations, handling, care, and purchasing costs.^{67,68} Consequently, alternative approaches, such as *in vitro* methods and computational models, have been employed to predict the BBB penetration ability of drug candidates.^{69,70}

In silico models are computational simulations used to predict the ability of a molecule to cross the BBB.⁷¹ Although they are fast and cost-effective, their accuracy in predicting the BBB permeability of a molecule depends on the validity of the underlying assumptions and the quality of the input data. Compared to *in vitro* and *in vivo* methods, *in silico* models generally have lower accuracy due to the complexity of the BBB and the difficulties in accurately modeling the BBB. However, these models can still be valuable tools for screening potential drug candidates and identifying molecules that are more likely to cross the BBB before investing resources in *in vitro* or *in vivo* experiments. Along with progress in algorithms and input data, the accuracy of *in silico* models for predicting BBB permeability is expected to improve.

In vitro models are important tools for studying the BBB and can be categorized into cell culture systems and non-cell-based models. Cell culture systems, including transwell systems, microfluidic devices, and three-dimensional (3D) cultures, provide controlled, reproducible conditions for studying the BBB. These models can offer valuable insights into the mechanisms underlying BBB permeability and drug transport across the BBB, enabling the development of more effective brain therapeutics.⁷²⁻⁷⁶

4.1. Cell-based *in vitro* BBB models

4.1.1. Validation of the cell-based models

The BBB is a highly selective semipermeable membrane formed by continuous ECs, with junctional proteins forming a key component of its integrity. BBB disruption can alter the balance among TJs, AJ proteins, MMPs, cell adhesion molecules, and various neuroinflammatory proteins. Therefore, developing models that enable early detection of BBB breakdown via protein biomarker assays to support targeted medicines is increasingly essential.⁷⁷ Before discussing models, it is necessary to define several

technical parameters to establish usable approaches for validation. These may include assessing EC TJ and AJ expression using real-time polymerase chain reaction (PCR) and Western blotting, as well as their functionality through transepithelial/transendothelial electrical resistance (TEER) and permeability assays. In addition, the evaluation of the expression and function of ATP-binding cassette (ABC) transporters, particularly P-glycoprotein (P-gp), through intracellular uptake assays or the crossing rate of specific substrates for P-gp, such as calcein-acetoxymethyl and rhodamine 123, will help validate cell-based models.

4.1.2. Molecular-based analysis: Gene expression and protein assays

Gene microarray technologies have been developed in recent decades to identify highly expressed BBB genes and BBB-enriched genes, including genes encoding TJs, AJs, and ABC transporters, which are exclusive to ECs and play a crucial role in BBB function. These genes can be detected using whole-brain gene microarrays. Various methods, such as western blotting, immunohistochemistry, enzyme-linked immunosorbent assay, and real-time PCR, are employed to detect these markers.⁷⁸

4.1.3. Functional assays to measure the integrity and permeability of *in vitro* barrier model systems

To validate *in vitro* BBB models at the functional level, paracellular transport and proper ABC transporter function have been evaluated by TEER measurements and permeability assays, respectively, along with measurements of ABC transporter efflux transport function (i.e., intracellular uptake or crossing rate).⁷⁸

- (i) TEER measurement: The TEER value⁹ is closely associated with barrier tightness.⁷⁹ In peripheral tissues, TEER values range from 2 to 20 $\Omega\cdot\text{cm}^2$, while for the BBB, TEER typically increases to 1,000–5,000 $\Omega\cdot\text{cm}^2$.⁸⁰ Hodgkin and Katz's⁸¹ theory posits that current flow leakage through vessel capillaries leads to a decrease in intracapillary voltage that follows an exponential decay pattern as the distance from the current source increases within a fixed length of the vein. The extent of the decrease in potential is influenced by the ionic permeability of the capillary membrane.⁸² TEER (R_m) is determined by several parameters, including the length constant (λ), the resistive index (r_i) of the blood, and the radius of the vessel (α), as shown in Equation (1):^{80,83}

$$R_m = r_i \lambda^2 2\pi\alpha \quad (1)$$

The two most widely used instruments for measuring TEER are the epithelial/endothelial volt ohmmeter

(EVOM) and the microelectrode array (MEA). EVOM is a traditional method in which a pair of electrodes is placed on either side of the cell culture membrane, and the instrument measures the small current and calculates the electrical resistance of the cell layer. This method measures the membrane's barrier function, expressed in $\Omega\cdot\text{cm}^2$. MEA measures cellular electrical activity by recording extracellular field potentials, which reflect ion currents flowing across the cell membrane. The basic instrument consists of a grid of small metal electrodes embedded in an insulating layer. When cells generate ion currents during normal activity, these currents propagate through the extracellular space and can be measured using the electrodes on the MEA. MEA has several advantages over EVOM. First, MEA enables real-time, continuous monitoring of TEER values, whereas EVOM only measures TEER at discrete time points. Second, MEAs allow measurements to be taken from multiple locations within the cell culture, providing a more representative picture of the overall TEER value. In contrast, EVOM measures TEER at a single location. Third, MEA is a non-invasive method that does not require physical contact with the cell culture, whereas EVOM requires electrodes inserted into the culture, which could damage cells and introduce variability into TEER measurements. Overall, the MEA provides more accurate and reliable information about the integrity of the cell model. These two instruments are illustrated schematically in Figure 4.

- (ii) Assessment of the permeability of *in vitro* barrier model systems: The permeability of tracer compounds through the barrier is a crucial parameter for evaluating the integrity of the paracellular and transcellular transport pathways in cell culture models.^{78,84} Tracer compounds act as indicators of barrier permeability, allowing researchers to assess the efficiency of barrier function under different experimental conditions.⁸⁵ *In vivo* models typically use Evans blue, lucifer yellow, and sodium fluorescein to measure permeability. These compounds are administered systemically and allowed to circulate in the bloodstream, after which they penetrate the cell monolayer and accumulate in the tissue of interest. *In vitro* models, on the other hand, use several tracer compounds, such as lucifer yellow and fluorescein isothiocyanate-dextran, to assess the permeability of the cell monolayer.^{78,86} These compounds are added to the apical or basolateral compartment of the cell culture, and their passage through the cell monolayer is monitored over time. The amount of tracer compound that passes through the cell monolayer and accumulates in the opposite compartment is then quantified to determine the barrier's permeability. Overall, using tracer

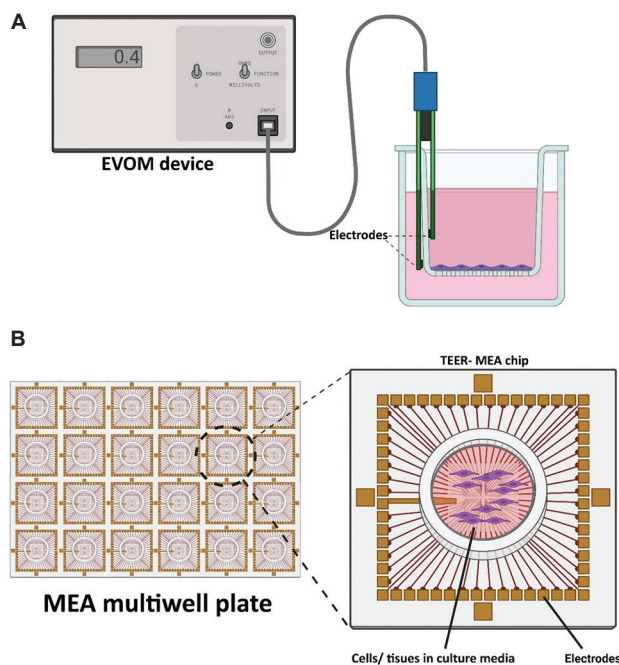


Figure 4. TEER measurement devices: EVOM and MEA Chips. (A) The EVOM device includes a specialized Ohmmeter and various microelectrodes, such as the STX2 electrode system. The device applies a small electrical current across the cell layer, and the voltage across the electrodes is measured. The TEER value is then calculated by multiplying the resistance by the surface area of the cell layer. (B) The TEER MEA chip consists of an array of microelectrodes that are embedded in the bottom of a culture plate, with different numbers of wells available. The electrodes on the MEA chip can be connected to the EVOM device using specialized cables. The MEA chip provides a high-throughput method for measuring TEER in multiple wells simultaneously. Created in BioRender. Aliakbari, F. (2026) <https://BioRender.com/1d7pa95>.

Abbreviations: EVOM: Epithelial/endothelial volt ohmmeter; MEA: Micro electrode array; TEER: Transepithelial/transendothelial electrical resistance.

compounds to assess permeability is a valuable tool for evaluating the integrity of cell culture barriers and assessing the effects of experimental conditions on barrier function.⁸⁶ It allows for the measurement of both paracellular and transcellular transport pathways and can be used in both *in vivo* and *in vitro* models.

Validating approaches for cell-based models, which are reviewed here, can be influenced by the types of cells and culture media utilized in the *in vitro* BBB cell system; both aspects are described in detail in the following sections.

4.1.4. Cell types used in cell culture models of the BBB

In 1980, the first *in vitro* BBB cell system was established using isolated cerebral capillary ECs.⁸⁷ One common *in vitro* model of the BBB involves a cell monolayer isolated from primary brain endothelial microvessels or immortalized brain endothelial microvessels with various adaptations.

Other *in vitro* models use cocultured cells under varying culture conditions to closely mimic the actual BBB. BBB coculture models have been developed using a combination of brain ECs with pericytes, astrocytes, and neurons to better approximate the anatomical and physiological complexity of the BBB.^{86,88} *In vitro* models of the BBB can be generated using various cell types, including primary cells, human or non-human EC lines, and stem cells.⁷⁹ Primary cells can be isolated from human brain tissue or animals, such as cows, pigs, rats, and mice. While human primary cells can be obtained from the postmortem brain within 14–24 h of death, ethical and legal considerations often limit their availability. In contrast, there are fewer ethical limitations when isolating primary cells from other animals, which can be obtained from embryos, fetal progenitors, newborns, or adult animals.^{89–91} Although primary cells closely resemble the *in vivo* state of the BBB, separating and purifying them can be complex, intricate, and time-consuming.^{92,93} In addition, ethical considerations can limit their availability. The number of passages of primary human BMECs is also limited due to their rapid senescence.⁹⁴ In contrast, the most commonly used cell lines for BBB models are derived from rodents (bEnd.3, bEnd.5, RBE4, cEND, cereBEND, PC12), cows (t-BBEC-117), pigs (PBMEC/C1-2), and humans (hCMEC/D3, human BMEC, SH-SY5Y, TY10, and BB19).^{95–97} Immortalized cell lines have unlimited passage numbers, high availability, and reproductive potential, with the ability to remain viable over numerous passages.^{14,98} They also enable the extraction of large amounts of protein or the consecutive expression of a gene without the need for a living animal. However, their different gene expression patterns from those of normal cells and changing characteristics after multiple passages could pose problems.⁹⁹ With the development of stem cell technology, primary and immortalized cell lines used for BBB modeling are being gradually replaced by stem cells. Stem cells are pluripotent cells that can differentiate into various mature somatic cell types.⁹⁹ Due to the limitations and challenges of using primary human cells in models, stem cells capable of differentiating into all cell types in the NVU are a valuable alternative to human *in vitro* BBB models.¹⁰⁰ Like primary cells, stem cells are derived from a living organism and can be continuously reproduced like immortalized cell lines.⁹⁹ Stem cells, including embryonic stem cells, fetal neural stem cells, induced pluripotent stem cells (iPSCs), and mesenchymal stem cells (MSCs), are generally derived from adult and embryonic or neonatal tissue sources.⁹⁵ An example is the use of neural progenitor cells (NPCs) derived from embryonic day 14, which can differentiate simultaneously into neurons, astrocytes, and oligodendrocytes. These cells can then be cocultured with human pluripotent stem

cell-derived BMECs to provide a barrier with a maximum TEER of $1,450 \Omega\text{-cm}^2$.¹⁰⁰ Despite the advantages of iPSCs in modeling the BBB, limitations in the maturation and differentiation processes of iPSC-derived cells, due to their physiologically relevant tissue microenvironment, may cause difficulties in their application as disease modeling.¹⁰¹ Moreover, their genetic instability and cell heterogeneity, as well as inconsistent manufacturing workflows preventing reproducibility, are the other challenges that limit their utilization as *in vitro* models.¹⁰²

Specific parameters must be verified to construct a valuable BBB model, including TEER, permeability, and the expression of particular proteins, such as TJ proteins. *In vitro* models strive to achieve conditions that closely resemble *in vivo* values. The TEER of some animal primary cell models of the BBB has been reported to be high. For example, some coculture models using astrocytes or pericytes extracted from rats have reached TEER values of $600 \Omega\text{-cm}^2$.¹⁰³ Higher values have also been reported using cells from cows and pigs (Table 3). In contrast, the highest TEER reported for immortalized cells was $800 \Omega\text{-cm}^2$, which is similar to that reported for the cEND cell line.⁹⁶ Butt *et al.*⁸⁰ reported that the highest TEER achieved from the pial vessels of rats at 21 days of gestation was $5,900 \Omega\text{-cm}^2$.

Notably, human cell lines or stem cell models can display high TEER values. For example, monocultures of human pluripotent stem cell-derived BMECs treated with retinoic acid can produce TEER values $>3,000 \Omega\text{-cm}^2$, and in coculture with pericytes using modified EC medium, TEER values can exceed $5,000 \Omega\text{-cm}^2$.¹⁰⁸ In 2017, Appelt-Menzel *et al.*⁷² developed a quadruple culture model based on four cell types: human induced pluripotent ECs, human iPSC-derived neural stem cells, astrocytes, and pericytes. They reported that the TEER of this model achieved $2,500 \Omega\text{-cm}^2$, and the permeability parameter of dextran (40 kDa) was approximately $0.0030 \pm 0.0004 \mu\text{M}/\text{min}$. In BBB models, pericytes decrease barrier permeability and

increase the TEER.¹⁰⁹ Several studies have shown that the phenotypic characteristics of mesenchymal cells are similar to those of pericytes. It has been suggested that MSCs possess leukocyte-like, active homing mechanisms involving adhesion molecules, chemokines, and proteases that enable transmigration under conditions of BBB damage and inflammation.^{110,111} MSCs can potentially improve BBB parameters, including TEER and permeability indices.¹¹² Therefore, MSCs could be a potential alternative to pericytes in *in vitro* models. Tian *et al.*¹¹² presented a model of the BBB using brain capillary ECs (mouse bEND.3 cells) cocultured with MSCs as a substitute for pericytes, and exhibiting MSCs compared to astrocytes and pericytes. They were able to construct a strong barrier and improve BBB properties.

In conclusion, the cell type is a critical factor determining the quality of *in vitro* cell-based BBB models and must be carefully considered during their design.

4.1.5. Improving cell-based *in vitro* models with a proper culture medium

Culture medium can significantly impact the characteristics of the BBB model. Researchers can create accurate and reliable BBB models by carefully selecting the appropriate culture medium and conditions. For example, TEER values are sensitive to the ionic composition of the culture medium.⁹ In addition, various components of the culture medium can affect the tightness of the barrier. When used at physiological concentrations, hydrocortisone can improve barrier properties in serum-free culture systems and improve BBB characteristics, including increasing and decreasing TEER and permeability.^{113,114} The addition of cyclic adenosine monophosphate has also been reported to improve BBB parameters.^{115,116} On the other hand, Vatine *et al.*¹¹⁷ demonstrated that personalized BBB chips with patient-derived iPSCs could distinguish different BBB parameters.

Table 3. Comparison of the TEER parameters of *in vitro* BBB models using primary cells extracted from different animals

Animal type	Culture type	TEER <i>in vitro</i> ($\Omega\text{-cm}^2$)	References
Pig	Monoculture	344±25	104
	Non-contact coculture (astrocyte/pericyte)	1,093±60/778±33	
	Contact coculture (astrocyte/pericyte)	1,123±89/831±29	
Pig	Monoculture	789±18	105
Rat	Monoculture	~150	106
	Coculture	~200	
	Coculture	~600	
Cow	Coculture (rat astrocyte)	Minimum: 261±26	107
		Maximum: 760±46	

Abbreviations: BBB: Blood-brain barrier; TEER: Transepithelial/transendothelial electrical resistance.

BBB coculture systems containing ECs and neural cells require fetal bovine serum (FBS).^{118,119} However, when culturing neurons in neurobasal media, the main issue is the atypical use of serum, which requires careful consideration of its effects on neuronal topology, especially synaptic arrangement. For example, Bang *et al.*¹²⁰ Investigated synapse arrangements under three conditions. Briefly, they observed that FBS is suitable for coculture, EC growth medium-cultured astrocytes are necessary for cell migration, and VEGF-A increases proliferation.¹²⁰

4.1.6. Static cell-based BBB model using Transwell inserts

The Transwell system is a cell culture system comprising two compartments separated by a semipermeable membrane. It typically consists of an insert with a permeable membrane placed into a cell culture plate well. The insert divides the well into two compartments: The apical and basolateral compartments. Cells are seeded onto the membrane and form a monolayer, creating a barrier between the two compartments. The system can be used to assess the permeability of the cell monolayer and to study the mechanisms of transport across the barrier. The Transwell system can be employed for multiple cell cultures and has numerous applications, including evaluating the effects of experimental conditions, such as drug treatments or disease states, on barrier function.^{69,70,86,121,122} A schematic of the Transwell system and its advantages and disadvantages is provided in Table 4.

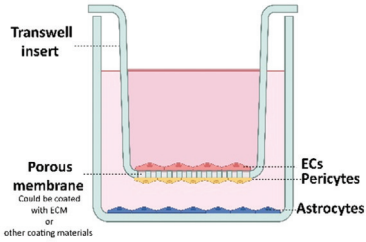
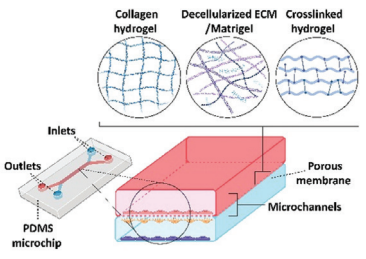
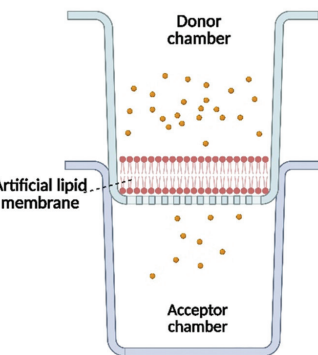
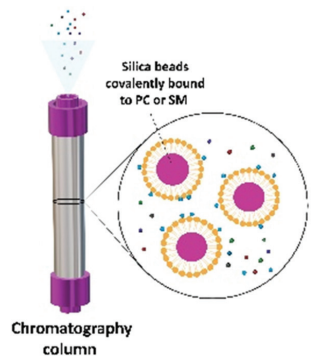
The use of a transwell system as a BBB model requires a microporous semipermeable filter membrane, which can be obtained commercially, e.g., from Corning. These filters are typically made of polycarbonate or polyethylene terephthalate materials, with pore sizes ranging from 0.4 to 8.0 μm . Alternatively, the membrane can be designed using tissue engineering techniques, such as fabricating a polyacrylonitrile electrospun nanofibrous membrane on a 3D-printed Transwell, to mimic the structure of the BM.^{123,124} The membrane pore size can vary depending on the intended application. For instance, a pore size of 0.4 μm is suitable for drug permeability screening, while 8 μm is preferred for transmigration investigations.^{86,125} Different proposed models, including mono- and multiculture models (co, tri-, and quadruple), can be used with microporous filter membranes. In a monoculture model, BMECs are cultured alone on the filter membrane, which facilitates permeability, proteomics, and genomics analyses.^{126,127} However, as this model lacks other components of the NVU (astrocytes, pericytes, and BM), TEER and paracellular permeability measurements may not reflect those of the *in vivo* BBB.¹²⁸ Multicultural models, on the other hand, can improve the physiological relevance of the BBB model.¹²⁹

In all BBB models, the type of cell used (primary, stem cell, or immortalized), the origin of the cell (rat, cow, pig, human, etc.), and the arrangement of cells in the model and their interactions with each other significantly affect gene expression and the formation of TJs, which in turn affects electrical resistance, permeability, and shear stress.¹³⁰ Table 5 summarizes the differences in the TEER and permeability resulting from different cell arrangements in the coculture Transwell system. Examples of multiculture Transwell systems include a system developed by Hutamekalin *et al.*,¹³¹ in which rat BMECs were cocultured with astrocytes, achieving an average TEER value of 200–300 $\Omega\cdot\text{cm}^2$ and a maximum TEER value of 600 $\Omega\cdot\text{cm}^2$. In another study, Smith *et al.*¹³² achieved a TEER of 900 $\Omega\cdot\text{cm}^2$ by coculturing porcine BMECs with the C6 astrogloma cell line. Several factors can improve TEER and permeability of *in vitro* cocultures, making them more similar to *in vivo* BBB models. These factors include using stem cells (iPSCs, MSCs) to replace primary cells, using retinoic acid to differentiate fetal stem cells into NPCs, modifying the ECM, using cell culture medium lacking basic FGF, and incorporating macrophages, astrocytes, and pericytes.^{108,115} These modifications can lead to a TEER > 5,000 $\Omega\cdot\text{cm}^2$, which is closer to the TEER observed in *in vivo* BBB models (above 1,000 $\Omega\cdot\text{cm}^2$ for mammalian BBB).¹³³ The Transwell system is easy to set up, use, and control. Therefore, it could be ideal for studying Michaelis-Menten-type kinetics of transport.¹³⁴ However, the lack of fluid flow and direct interaction between cells can create challenges in this model.^{127,129} Transwell-generated ECs may exhibit an irregular growth pattern, which can impair the proper formation of TJs between cells, leading to an “edge effect.”¹³⁵ The “edge effect” is caused by the irregular growth pattern of the ECs on the Transwell membrane, resulting in the improper formation of TJs at the edges of the membrane. This can lead to reduced barrier function and increased paracellular permeability at the edges of the membrane, potentially affecting the accuracy and reliability of the experimental results obtained from the Transwell system.

4.1.7. Modeling the BBB with microfluidic platforms: Simulating a dynamic microenvironment

Among *in vitro* models for studying the BBB, multicellular culture models are known for their ability to recapitulate the complex physiological response of the BBB through critical interactions between different cell types in the NVU.^{142,143} In addition to cellular interactions, the activity of the BBB is affected by various environmental factors, including shear stress, oxygen levels, inflammatory cytokines, pH, neurotransmitters, and drug interactions.^{144–146} Understanding how these factors affect the BBB is essential

Table 4. Schematic overview of *in vitro* BBB models, including their advantages and disadvantages

BBB model	Design	Description	Advantages	Disadvantages
Transwell		<ul style="list-style-type: none"> - A 2D model capable of coculturing different types of NVU cells - Static 	<ul style="list-style-type: none"> - Consistent - Easily operated - Reproducibility of results - Represent active transport - Commercial accessibility - Provide proper conditions to resemble NVU in terms of the coculture ability - Less time-consuming and less costly 	<ul style="list-style-type: none"> - No shear stress - Limited complexity - The rigid surface of the insert - Rapid loss of BBB characteristics - The indirect connection between NVU cells
Microfluidic		<ul style="list-style-type: none"> - 2D and 3D cocultures on a microchip in a fluid medium - Dynamic 	<ul style="list-style-type: none"> - Represent active transport - Imitates BBB in small scales and more closely to the actual <i>in vivo</i> brain anatomy - Enables the effect of shear stress; shear stress is applied and can be controlled - Continuous media exchange - Desirable representation of the 3D structure of NVU - The simplicity of providing materials, e.g., drugs and media, and cells into the channels 	<ul style="list-style-type: none"> - Technically complex - No visualization of the intraluminal compartment; monitoring the uniformity of the culturing system could be challenging - Limited control; difficult to inspect contamination - Difficult to set up
PAMPA		<ul style="list-style-type: none"> - A type of CFMPA that contains an artificial, bio or non-biological membrane between two chambers 	<ul style="list-style-type: none"> - A high-throughput drug permeability assay based on passive transport 	<ul style="list-style-type: none"> - Suitable only for the early stages of drug screening - Unable to represent active transport - Weaker selective permeability than natural cell membranes
IAM		<ul style="list-style-type: none"> - A type of CFMPA made of a high-performance chromatography column with a solid phase containing covalently bound silica-(phosphor) lipids 	<ul style="list-style-type: none"> - A high-throughput method for testing drug affinity to cell membranes based on lipophilicity 	<ul style="list-style-type: none"> - Restricted replication of the native cell membranes and their incorporated receptors

Source: Created in BioRender. Aliakbari, F. (2026) <https://BioRender.com/erpo4jb>.

Abbreviations: 2D: Two-dimensional; 3D: Three-dimensional; BBB: Blood-brain barrier; CFMPA: Cell-free models for permeability assay;

IAM: Immobilized artificial membrane; NVU: Neuro-vascular unit; PAMPA: Parallel artificial membrane permeability assay.

Table 5. Different arrangements in multi-cultural models using the Transwell system

Top of filter	Lower side of the filter	Bottom of the well	Species/cell type	TEER/permeability parameters	References
A mixture of pericytes and astrocytes	-	Endothelial cells	2-week-old rats/primary cell	329 Ω ·cm ²	136
Endothelial cells	-	Mixture of glial cells	Bovine, rat/primary cell (bovine endothelial cell, glial cell from newborn rat)	0.51×10 ⁻³ cm/min (LY molecule)	137
	-	Mixture of glial cells and pericytes	Bovine, rat/primary cell (bovine endothelial cell and bovine pericyte, newborn rat glial cell)	0.30±0.01×10 ⁻³ cm/min (LY molecule)	138
	Pericytes	Astrocytes	3-week-old rat/primary cells (rat endothelial cells, neonatal rat astrocyte cells, rat pericytes)	354±15 Ω ·cm ² ; 3.9±0.2×10 ⁻⁶ cm/s (sodium fluorescein)	139
	-		2-week-old rats/primary cell	300 Ω ·cm ²	131
	-		Bovine/primary cell (bovine endothelial cell, newborn rat astrocyte)	600 Ω ·cm ²	140
	-		Porcine/C6 glioma cell line	900 Ω ·cm ²	132
	-	Pericytes and astrocytes (primary human brain pericytes, human astrocytes, neurons derived from human neural progenitor cells)	Human/stem cell line hCMECs	3,500 Ω ·cm ²	108
	Astrocytes	-	Bovine, rat/primary cells (rat astrocyte/bovine endothelial cell)	661±48 Ω ·cm ²	141
Pericytes together with endothelial cell	-	Glial cell	Bovine, rat/primary cell (bovine endothelial cell and bovine pericyte, newborn rat glial cell)	0.41±0.05×10 ⁻³ cm/min (LY molecule)	138

Abbreviations: hCMECs: human cerebral microvascular endothelial cells; LY: Lucifer yellow; TEER: Transepithelial/transendothelial electrical resistance.

for developing accurate *in vitro* models. Microfluidic systems can provide dynamic models that better mimic the *in vivo* BBB microenvironment, allowing for the study of the effects of these environmental factors on BBB function in health and disease, as well as drug screening.

4.1.8. Overview of microfluidic devices used for modeling the BBB

Organ-on-chip platforms are 3D-engineered microscale systems that fabricate multicellular structures, tissue-tissue interfaces, mechanical forces, physicochemical microenvironments, and vascular perfusion to achieve tissue and organ functionality. Various types of organ-

on-chips can be used for BBB modeling and validity assessment, including continuous luminal perfusion, real-time TEER monitoring, live-cell imaging for permeability measurements, and metabolic pathway analysis.¹⁴⁷⁻¹⁵² Studies using these platforms have demonstrated their suitability as BBB models.

Microfluidic devices designed for BBB models typically consist of one or more chips that can be used to fabricate different components of the NVU system. A schematic of microfluidic devices and their advantages and disadvantages is provided in Table 4. Microfluidic devices have been developed for modeling the BBB, with

each machine offering unique advantages. Well-known microfluidic devices include the following:

- (i) BBB primitive models consist of two microchannels separated by a porous polycarbonate or polydimethylsiloxane membrane with a 0.4 μm pore size. The vascular compartment is used to culture ECs, while the brain compartment is usually used to culture astrocytes.¹⁵³ These models accurately measure TEER, permeability, and other BBB properties, replicating *in vivo* conditions and providing a reliable system for personalized medicine. Hence, these personalized medicine models have facilitated the discovery of BBB alterations in various diseases^{117,154} and drug permeability screening in drug development.¹⁵⁵
- (ii) To analyze the role of each cell type in the NVU, a coupled system can be created by placing a brain chip with a neural cell between two BBB chips, an influx BBB chip, and an efflux BBB chip. Maoz *et al.*¹⁵² designed a system to mimic the flow of cerebrospinal fluid through the neuronal medium and to identify substances that do not leave the brain via the output. The bloodstream medium entering from one side of the BBB represents substances entering the brain parenchyma, and materials obtained from the output of the last chip (BBB efflux) indicate materials that can leave the brain.
- (iii) Plate-based microfluidic platforms allow automated high-throughput testing with high-content images.¹⁵⁶ However, adding cells or biomaterials to culture wells during cell culture is impossible in these devices, and circulating non-adherent cells are another essential feature of “organ-on-chip” applications.¹⁵⁷ To simulate the BBB, Koo *et al.*¹⁴³ constructed a two-channel apparatus that seeded neuroblastoma cells, astrocytes, and microglia in a gel-cell matrix as the brain compartment and cultured a monolayer of ECs on the other side.
- (iv) The vessel-like microfluidic channel allows for multiple applications in just one chip. Cho *et al.*¹⁵⁰ designed a tube-like tetrahedral microfluidic channel to culture a monolayer of ECs on each side, thereby mimicking the BBB, for various assays.
- (v) Pulsed electric fields (PEFs) can be used to increase the transcellular permeability of the BBB through electroporation, which leads to alterations in the membrane potential and finally the creation of nanoscale aqueous pores in the membrane and disruption of BBB integrity. Bonakdar *et al.*¹⁵⁸ provided a gradient platform along its length to exert different PEFs on cells in each section. This platform delivered graded electrical pulses to determine the

threshold of electrical strength on BBB cells, and the cells’ viability was then assessed. Their study showed that 8–10 pulses are more applicable for drug delivery because no cell death was observed for electric fields <400 V/cm (Table 6). The orientation of cells on the plate is also a critical parameter, as cells oriented parallel to the electric field showed greater resistance than those oriented perpendicular to it.

4.1.9. Enhancing *in vitro* barrier formation in BBB models through cell-matrix interactions

The incorporation of natural endogenous decellularized ECM derived from tissues or cells has led to promising results in improving *in vitro* barrier formation.^{160,161} For example, Zobel *et al.*¹⁶² designed a BBB model of microvascular ECs cultured on layers of decellularized BM derived from pericytes and astrocytes, demonstrating increased TJ expression and TEER levels, particularly with the two-layer BM combination that closely mimicked *in vivo* conditions.

It is essential to simulate the natural features of the NVU as much as possible to design an accurate *in vitro* BBB model. Hydrogels (polymers with high water content and structural and biochemical resemblance to the native ECM) are often used for this purpose. They can be classified into three groups: (i) natural hydrogels consisting of tissue or cell-derived BM/ECM extracts (e.g., matrigel, collagen type I), (ii) synthetic biomaterials, such as peptide hydrogels, and (iii) semisynthetic hydrogels, which are modified combinations of natural and synthetic hydrogels.¹⁶³

Matrigel, a commercially available laminin-rich BM extract derived from the Engelbreth-Holm-Swarm tumor, is a commonly used resource in cell culture.^{164,165} However, batch-to-batch variation and animal origin can affect reproducibility and trigger immune responses in human BBB models used for drug screening.¹⁶⁶ Human-based equivalents of Matrigel, such as MaxGel[®], are also available commercially.

Natural bioactive hydrogels, such as collagen, gelatin, fibronectin, and laminins, possess integrin-binding motifs and can be recognized and degraded by MMPs. Synthetic hydrogels lack these properties but offer advantages for maintaining a stable and controllable structure. Synthetic peptide hydrogels can be functionalized to provide cell adhesion domains. Combining several hydrogels based on natural and synthetic materials can compensate for the limitations of each material, such as covalently crosslinking silk fibroin proteins with hyaluronic acid to enhance the biomechanical properties of the fabricated hydrogel.¹⁶⁷

Microfluidic BBB models often use hydrogels in built-in “gel channels” to optimize model efficiency. Two or more ECM components can be used together in a mixture or in

Table 6. Summary of studies using microfluidic systems to model the BBB

The type of changes performed in the microfluidic system	Study aim	The detail of changes	Conclusions	References
Pumpless platform	Long-term maintenance of the BBB structure for the drug permeability study	Fluid delivery via gravity on a tilted rocking platform and recirculation by changing tilt direction	Maintains high TEER value for at least 10 days	155
		TEER value	4,399 ± 242 Ω·cm ²	
		Permeability	FITC-dextran 4 kDa, 20 kDa, 70 kDa	
			10 ⁻⁷ ~ 10 ⁻⁸ cm/s	
		Caffeine (rapid penetration)	4.85 ± 1.84 × 10 ⁻⁴ cm/s	
		Cimetidine (moderate penetration)	1.11 ± 0.09 × 10 ⁻⁶ cm/s	
iPSC (iBMEC)-based model of disease	Organ-specific disease modeling	HD-iBMECs	Enhance permeability of the HD BBB-Chip	117
		MCT8 deficiency	Lower transport of T ₃ from blood to the brain	
Changes to the supplement	Improve the number of synaptic connections	NBM + B27	8.60 ± 1.50	120
		NBM + 2% FBS	9.20 ± 0.84	
		EGM	3.49 ± 0.37	
Changes in the media composition	Area occupied by vascular network	EGM/NBMFBS	0.0881 ± 0.0015 μm ²	
		EGM/EGM	0.0876 ± 0.0016 μm ²	
		5:5 mixed/5:5 mixed	0.0411 ± 0.0025 μm ²	
	Area occupied by astrocytes	EGM/NBMFBS	0.0542 ± 0.0010 μm ²	
		EGM/EGM	0.0393 ± 0.0008 μm ²	
		5:5 mixed/5:5 mixed	0.0529 ± 0.0029 μm ²	
	Permeability coefficients with 20 kDa FITC-dextran	EGM/none	(n = 9) 1.85 ± 0.20 × 10 ⁻⁶ cm/s	
		EGM/EGM	(n = 14) 0.65 ± 0.08 × 10 ⁻⁶ cm/s	
		EGM/NBMFBS	(n = 13) 0.45 ± 0.11 × 10 ⁻⁶ cm/s	
	Permeability coefficients with 70 kDa FITC-dextran	EGM/none	(n = 12) 1.39 ± 0.19 × 10 ⁻⁶ cm/s	
		EGM/EGM	(n = 12) 0.60 ± 0.12 × 10 ⁻⁶ cm/s	
		EGM/NBMFBS	(n = 20) 0.36 ± 0.05 × 10 ⁻⁶ cm/s	
Making a gradient in channel length and applying different pulses	Cell death	10 pulses	0–40%	158
		30, 90 pulses	5–100%	
Tube-like structure	Neuroinflammation	Treated with TNF-α	Increase several cytokines	159
			Decrease or even deplete ZO-1 proteins	
			Increase the BBB permeability	

(Cont'd...)

Table 6. (Continued)

The type of changes performed in the microfluidic system	Study aim	The detail of changes	Conclusions	References
Coupled NVU system	Ischemia model and oxidative stress	Treated with the OGD procedure and reoxygenation	2.8-fold elevated level of ROS	152
			3.0-fold elevated level of p-MLC	
			Reduction of ZO-1 expression level	
	Restore BBB integrity	3 h after adding antioxidant, edaravone, and a ROCK inhibitor, Y-27632, and reoxygenation	7–10% elevation of ZO-1 expression level	
		6 h after adding antioxidant, edaravone, and a ROCK inhibitor, Y-27632, and reoxygenation	1% increase in cellular death	
			5% decrease in ZO-1 marker levels	
			Significant changes in protein expression in the endothelium, perivascular, and neurons	
	Roles of individual cell types in NVU	Coupled system	Downregulation of vesicular transport processes in vascular endothelium	
			Less proliferative and less migratory	
	Utility of the NVU system for drug-modeling studies	Administration of 1.5 mM methamphetamine into the vascular channel of the BBB influx chip	Vascular and perivascular tissues maintain high metabolic activity	
			Reversible breakdown in the BBB influx chip and an increase in permeability	
Coupled NVU system	Metabolic coupling among various cell populations	Supply C13-labeled glucose exclusively to the vascular channel of the BBB influx chip	Significant alteration in components of specific pathways	152
			Perivascular cells have a higher number and variety of metabolic alterations	
	Metabolic coupling among various cell populations	Supply C13-labeled glucose exclusively to the vascular channel of the BBB influx chip	Glucose transport across the BBB influx	
			Glycolysis occurred in all compartments of the NVU system	
			In the brain chip neural, glycolysis is likely to happen in astrocytes	
			Glutamine synthesis with astrocyte and endothelial and observed in all compartments	
			GABA only produced by the cells of the brain chip	
			Free exogenous pyruvate and lactate contribute to neurotransmitter synthesis	
			Metabolites secreted from BBB cells help brain cells to synthesize glutamine	

Abbreviations: BBB: Blood-brain barrier; EGM: Endothelial cell growth medium; FBS: Fetal bovine serum; FITC-dextran: fluorescein isothiocyanate-dextran; GABA: Gamma aminobutyric acid; HD: Huntington's disease; iBMEC: Induced brain microvascular endothelial cell; iPSCs: Induced pluripotent stem cells; MCT8: Monocarboxylate transporter 8; NBM: Neurobasal media; NBMFBS: Neurobasal media + 2% fetal bovine serum; NVU: Neuro-vascular unit; OGD: Oxygen glucose deprivation; p-MLC: Phosphorylation of the myosin light chain; ROCK inhibitor: Rho-kinase inhibitors; ROS: Reactive oxygen species; TEER: Transepithelial/transendothelial electrical resistance; TNF: Tumor necrosis factor; ZO: Zonula occludens.

different chambers of a microfluidic device to enhance cell attachment, such as by coating cells with or encapsulating them in ECM.^{168,169} Direct 3D bioprinting, which

involves layer-by-layer deposition of cell-laden hydrogel biomaterials, is another valuable platform for BBB models that has attracted increasing interest in the past decade.¹⁷⁰

Overall, the choice of culture medium or biomaterials critically determines BBB model fidelity. Examples of biomaterials utilized as BMs in designing BBB models and brain tissue engineering are presented in [Table 7](#).

4.2. Cell-free models for permeability assays (CFMPAs)

Cell-free models can be implemented in the early stages of drug design to simulate biological membranes without living cells, providing a high-throughput screening tool.

Table 7. Examples of important biomaterials utilized in BBB design

Materials	Hydrogel type	Source/composition	BBB/NVU model	Observed effects	References
Matrigel	Natural	Mouse EHS tumor tissue-derived BME \pm growth factors	BBB-on-chip	- Promotes cell adhesion, forming capillary-like structures	171,172
Collagen I	Natural	Animal tissue-derived (rat tail, extracted by acid solubilization; bovine skin/porcine skin, extracted by pepsin digestion)	BBB Transwell model (collagen I-coated, aligned PCL nanofibers)	- Enhances endothelial barrier integrity and uniformity in junction formation - <i>In vivo</i> -resembling cell alignment in endothelial cells	173,174
Hyaluronic acid	Natural	ECM polysaccharide	BBB spheroids (tri-culture hybrid)	- Promotion of spheroid fusion	175
Fibrin	Natural	Polymerization of fibrinogen by thrombin	NVU microfluidic model (fibrin-matrigel mixed gel)	- Promoting differentiation of neural stem cells into neurons - Promoting neurite extension	172
Gelatin methacrylate	Semi-synthetic	Addition of methacrylic anhydride to the amine groups of gelatin	Micro-patterned substrates/ cell-encapsulated endothelial microvessels	- Successful proliferation, elongation, and migration of HUVECs on the surface of, or embedded in, the hydrogel	176,177
Agarose-collagen composite	Semi-synthetic	Multilayered hydrogel structures	3D-bioprinted molds	- Maximizes viability of cultured neural and endothelial cells - Strong expression of TJs and elevation of TEER value by HMECs - Suitable for both 2D and 3D cell culture	178
PEG	Synthetic	PEG (hydrophilic polymer of ethylene oxide macromolecules) cross-linked with MMP-degradable and integrin-binding peptides	Transwell neural tissue model	- Produces a reproducible, uniform neural tissue construct	179
		PEG-maleimide with integrin-binding peptides and PEG-dithiol with MMP-degradable peptides	Astrocytes cultured in hydrogels to investigate astrocyte activation	- Creates an environment allowing control and maintenance of astrocyte quiescence with minimal activation	180

Abbreviations: 2D: Two-dimensional; 3D: Three-dimensional; BBB: Blood-brain barrier; BME: Basement membrane extract; ECM: Extracellular matrix; EHS: Engelbreth-Holm-Swarm; HMECs: Human mammary epithelial cells; HUVEC: Human umbilical vein endothelial cell; MMP: Matrix metalloproteinase; NVU: Neurovascular unit; PCL: Polycaprolactone; PEG: Polyethylene glycol; TEER: Transepithelial/transendothelial electrical resistance; TJ: Tight junction.

These models, known as CFMPAs, measure only the permeability of the compounds of interest. They can be associated with *in vitro* or *in silico* models of targeted cell cultures, including vascular ECs, to compensate for active transport or efflux pathways.

4.2.1. Simulation criteria for *in vitro* models

Although simulating biological membranes may seem straightforward, it is not trivial. Several parameters should be considered when designing *in vitro* cell-free models. One of the most important parameters is the lipid composition of the artificial membrane, which includes various phospholipids and sphingomyelins (SMs) that affect the membrane's fluidity and rigidity.⁷⁵ The endothelial lipid composition of different organisms and cell types is summarized in Table 8. In addition, the lipid composition of the EC plasma membrane often differs between the inner and outer layers. For example, in terms of the distribution of the main lipid head groups, phosphatidylcholines (PCs), SM, and gangliosides are predominant in the outer leaflet, while in the inner layer of biological membranes, phosphatidylethanolamine (PE), phosphatidylserine (PS), and other charged lipids are prevalent.¹⁸¹ The composition of lipids in the apical and basolateral plasma membranes can also influence drug absorption. Table 9 summarizes the differences in

lipid composition between the apical and basolateral sides of porcine brain capillary ECs.

Furthermore, the membrane charge differs between the BBB and the peripheral system. Brain capillary ECs have more anionic membranes than peripheral system ECs and could be a critical factor in maintaining homeostasis and attracting cationic materials.¹⁸⁵

Another parameter worth considering when designing *in vitro* models is the unstirred water layer, which particularly affects the drug permeability of highly lipophilic molecules,^{186,187} while the hydrocarbon layer in the membrane serves as the single rate-limiting barrier for hydrophilic molecules.¹⁸⁸ Indeed, a potential barrier has been created for lipophilic molecules due to the aqueous diffusion layer adjacent to the membrane.

4.2.2. Essential aspects of membrane elements in cell-free model simulation

When designing non-cell-based models that closely resemble the BBB membrane structure, it is essential to consider differences in SM and PC levels between the apical and basolateral membranes, as well as the significant differences in the ratio of the BV system to the peripheral vascular system (as discussed in the previous sections).^{75,189} A brief comparison of their structures helps clarify their functional roles.

Table 8. Lipid compositions in different organisms and cell types (values in mol %)

Lipid class	Human umbilical artery endothelial cell ¹⁸²	Human umbilical vein endothelial cell ¹⁸²	Human brain endothelial cell ¹⁸³	Bovine brain endothelial cell ¹⁸³	Porcine brain endothelial cell ¹⁸⁴
Phosphatidylcholine	49.0 ± 0.1	50.5 ± 0.1	33.2 ± 0.2	32.1 ± 0.4	28.7 ± 1.4
Sphingomyelin	5.9 ± 0.1	6.7 ± 0.1	17.0 ± 0.1	20.9 ± 0.2	13.4 ± 0.7
Phosphatidylserine	9.0 ± 0.2	9.1 ± 0.2	10.7 ± 0.1	10.6 ± 0.1	6.8 ± 0.7
Phosphatidylinositol	6.0 ± 0.3	5.9 ± 0.4	4.8 ± 0.2	4.5 ± 0.2	5.5 ± 1.3
Phosphatidylethanolamine	28.1 ± 0.3	25.5 ± 0.4	25.2 ± 0.4	23.9 ± 0.3	22.8 ± 1.6

Note: Only major lipid classes are listed; minor components were omitted; therefore, totals may not equal 100%.

Table 9. Lipid composition in the apical and basolateral plasma membranes of porcine brain capillary endothelial cells (values given in mol %) ¹⁸⁴

Lipid class	Apical plasma membrane	Basolateral plasma membrane
Phosphatidylcholine	21.3 ± 2.5	15.0 ± 0.9
Sphingomyelin	17.5 ± 2.1	23.0 ± 1.2
Phosphatidylserine	8.3 ± 1.2	10.1 ± 1.3
Phosphatidylinositol	2.7 ± 0.8	1.7 ± 0.9
Phosphatidylethanolamine	20.8 ± 1.3	19.8 ± 1.9
Total phospholipids	70.6	69.6
Cholesterol	28.3 ± 4.5	28.8 ± 4.4
Glucosylceramide	0.3 ± 0.2	0.8 ± 0.1
Gangliosides	0.8 ± 0.2	0.7 ± 0.2

The physiological roles of SM can be divided into two categories: Its structural role in cell membranes and its biological role as a pre-cursor to metabolites, such as ceramide and sphingosine. One essential aspect of SM function in the cell membrane structure concerns its physical role, which encompasses the structural differences between PCs and SMs and their functional implications. PCs generally consist of glycerol attached to two fatty acids (usually saturated or unsaturated) at the sn-1 or sn-2 position, respectively, and phosphorylcholine attached to the third carbon.^{190,191} On the other hand, SM consists of a sphingosine base that binds phosphorylcholine and a fatty acid.¹⁹¹ PCs and SMs have similar structures, in which the sn-1,2-diacylglycerol in PC is replaced by N-acylsphingosine (ceramide) in SM.¹⁹²

The structural differences between PCs and SMs impact their phase behavior. Below physiological temperatures, PC and SM bilayers are in a fluid state due to the presence of cis double bonds in one of the PC chains, while at physiological temperatures, SM bilayers are in a gel-like phase due to the SM-saturated amide-linked chain.¹⁹³⁻¹⁹⁷ Moreover, the 3-hydroxyl group and the 4,5-trans double bond in the sphingoid chain of SM play various roles under different conditions, including effects on hydration and HB with adjacent water molecules and the formation of interfacial water and lipids via intra- and intermolecular hydrogen bonds. In addition, 4,5-trans double bonds contribute to gel-phase packing.¹⁹⁷ Intra- and intermolecular hydrogen bonds produce more vertical phosphocholine head groups and intermolecular cohesion, resulting in SM molecules packing tightly in an amorphous, irregular arrangement, with a smaller area per lipid. This HB promotes greater cohesive strength and less rigidity than PC.¹⁹⁷ In brief, SM provides more tightness with accompanying flexibility, which is a characteristic of the BBB.

4.2.3. Types of CFMPAs

Several types of CFMPAs have been used to simulate drug permeability. The parallel artificial membrane permeability assay (PAMPA)¹⁹⁸ and immobilized artificial membrane (IAM)¹⁹⁹ are the most commonly used and most reliable CFMPA methods.

- PAMPA

The PAMPA is a screening assay that measures the passive permeability of compounds across artificial membranes of biological or non-biological origin. The assay consists of membranes located between two chambers as donors and acceptors. The first report on the construction of an artificial membrane for assessing drug absorption was performed in 1996 by Kansy *et al.*,²⁰⁰ who dissolved egg lecithin in n-dodecane and coated it with

a hydrophobic filter material to measure gastrointestinal absorption of oral drugs. Over several years, to develop better models with greater similarity to BBB parameters, various artificial membranes have been developed as commercial PAMPA models, such as the PAMPA BBB porcine polar brain lipid (PBL) model, which is applicable for predicting the BBB permeability of compounds. In 2014, Campbell *et al.*⁷⁵ Compared three PBL-PAMPA models containing crude extract from a whole pig brain with human brain microvessel lipids and microvessel lipids plus cholesterol to evaluate the effects of lipid components on drug permeability. They demonstrated that changes in lipids affect the permeability of compounds with different structures.

Several commercial standardized PAMPA plates are available, including multiscreen polyvinylidene difluoride 96-well plates and transporter receiver plates from Millipore (USA). Different types of lipids can also be purchased from Avanti Polar Lipids (USA) or Sigma-Aldrich (USA). Table 10 summarizes the characteristics of different PAMPA membranes, including the lipid components, solvent types, support materials, dissolving material percentages, and their applications. For instance, the commercial PAMPA membrane from Avanti Polar Lipids contains 33.1% PE, 18.5% PS, 12.6% PC, 0.8% phosphatidic acid, 4.1% phosphatidylinositol, and 30.9% other components, including cerebroside, sulfatides, and pigments.²⁰¹ A schematic of the PAMPA model and its advantages and disadvantages is provided in Table 4.

As mentioned previously, CFMPAs can measure the passive permeability of compounds and investigate their active transport. It is essential to link cell-free models to *in vitro* (cell-based models that represent ABC transporters, such as P-gp) or *in silico* studies to increase the model's validity.^{187,209} In this regard, Mensch *et al.*¹⁸⁷ analyzed the Caco-2 efflux ratios of several compounds as active-transporter measurements in addition to their effective permeability through the PAMPA-BBB model.

- IAM (high-performance liquid chromatography column [HPLC])

Lipophilicity is an essential factor in drug permeability. The IAM method is an HPLC method that measures the amphipathic characteristics of biological membranes and thus permeability. The IAM method uses a chromatographic column as a stationary phase, which contains solid support such as silica that is covalently bonded to either octadecyl (ODS) or phospholipids (such as IAM-PC) to mimic biological membranes (Table 4). A solute or buffer is used as the aqueous mobile phase. ODS silica retains analytes based on hydrophobicity and is suitable for hydrophobic compounds,²¹⁰ while

Table 10. Different PAMPA models used in different studies

Artificial membrane	Lipids (native extract or synthetic lipid)	Solvent	Filter support	Percentage lipid to solvent (W/V)	Targeting application	References
PAMPA	Egg lecithin	N-dodecane	Hydrophobic filter material	10%	Prediction of oral absorption via the GIT	200
Biomimetic PAMPA combined with the paracellular pathway model based on the Renkin function	Mixture of lipid solution (PC, PE, PS, PI, and CHO)	Organic solvent (1,7-octadiene)	PVDF	PC, PE: 0.8%; PS, PI: 0.2%; CHO: 1%; 1,7-octadiene: 97%	Prediction of oral absorption via the GIT	202
Hexadecane membrane-PAMPA	Hexadecane (without lipid extraction or synthetic lipids)	Hexane	Isopore, polycarbonate (Teflon acceptor plate)	5%	Prediction of oral absorption via the GIT	203
DOPC-PAMPA	DOPC	Dodecane	PVDF, 125 µm microfilter disc	2%	Prediction of oral absorption via the GIT (pH range and determining UWL permeability)	188
DOPC-PAMPA	DOPC	Dodecane	PVDF, 125 µm microfilter disc	2%	Prediction of oral absorption via the GIT (to construct a new LFER, and hence for straightforward prediction from the molecular structure)	204
PAMPA-black lipid membrane	Dioleoylphosphatidylcholine	Dodecane	PVDF	2%	Prediction of BBB passive penetration	187
Double sink-PAMPA and PAMPA-GIT (commercial)	GIT lipid solution, soy lecithin, mixture of phospholipid (PC, PE, PI, phosphatidic acid, lyso-PC, triglycerides)	Dodecane	PVDF	20%	Prediction of oral absorption via the GIT	187
PBL-PAMPA (commercial)	Porcine polar whole-brain lipid, mixture of phospholipid (PC, PE, PI, PS, phosphatidic acid)	Dodecane	PVDF	2%	Prediction of BBB passive penetration	187
PAMPA-BBB-UWL (with a mechanical stirring apparatus)	Porcine PBL, donor wells contained a coated magnetic stirrer	Dodecane	PVDF	2%	Prediction of BBB passive penetration	187
PAMPA-black lipid membrane	Dioleoylphosphatidylcholine	Dodecane	PVDF	2%	Prediction of BBB passive penetration	186
Double sink-PAMPA	GIT lipid solution soy lecithin	Dodecane	PVDF	20%	Prediction of BBB passive penetration	186
PAMPA-BBB	Porcine PBL	Dodecane	PVDF	2%	Prediction of BBB passive penetration	186
PAMPA-BBB-UWL (with a mechanical stirring apparatus)	Porcine PBL, donor wells contained a coated magnetic stirrer	Dodecane	PVDF	2%	Prediction of BBB passive penetration	186
Skin PAMPA model	30% isopropyl myristate-70% silicone	N-hexane	PVDF	35% (v/v)	Prediction of human skin permeability	205

(Cont'd...)

Table 10. (Continued)

Artificial membrane	Lipids (native extract or synthetic lipid)	Solvent	Filter support	Percentage lipid to solvent (W/V)	Targeting application	References
PAMPA	L- α -PC from soybean	N-dodecane	Hydrophobic filter	2%, 10%, 20%	Prediction of oral absorption via the GIT	206
PBL-PAMPA	Porcine brain lipid	Dodecane	PVDF		Prediction of BBB passive penetration	207
PAMPA-PC lipid membrane model	L- α -PC	Dodecane	PVDF	2%	Prediction of BBB passive penetration	207
PBL-PAMPA (commercial)	Porcine polar whole-brain lipid	Anhydrous dodecane	PVDF	2%	Prediction of BBB passive penetration	75
Microvessel lipid	Microvessel lipid	Anhydrous dodecane	PVDF	2%	Prediction of BBB passive penetration	75
Microvessel lipid and CHO	Microvessel lipid and CHO	Anhydrous dodecane	PVDF	2%	Prediction of BBB passive penetration	75
Skin PAMPA	Lipid mixture (ceramides, stearic acid, CHO, silicone oil)	Lipophilic solvents (non-aqueous solvents and complex, emulsion-type formulations)	Teflon filter		Prediction of human skin permeability	208

Abbreviations: BBB: Blood-brain barrier; CHO: Cholesterol; DOPC: 1,2-dioleoyl-sn-glycero-3phosphocholine; GIT: Gastrointestinal tract; LFER: Linear free energy relationship; PAMPA: Parallel artificial membrane permeability assay; PBL: Polar brain lipid; PC: Phosphatidylcholine; PE: Phosphatidylethanolamine; PI: Phosphatidylinositol; PS: Phosphatidylserine; PVDF: Polyvinylidene difluoride; UWL: Unstirred water layer.

IAM-PC simulates a biological membrane by providing hydrophobic, ion-pairing, and hydrogen-bonding interactions.^{189,211} IAM-PC closely resembles a blood vessel, with a monolayer of phospholipids bound to the amphipathic propylamine-silica basement. However, residual propylamine groups may remain free, creating a basic microsubsurface in IAM-PC columns.^{189,212}

To overcome this problem, several modifications to IAMs have been made. PCs have been developed, such as end-capping residual amine groups with methylglycolate (MG) in IAM-PC-MG columns, and using decanoic anhydrides (DD) and propionic anhydrides (DD2) to end-cap IAM-PC columns in IAM-PC-DD and IAM-PC-DD2, respectively.^{189,212} Another challenge is that the cell membranes of endothelial vessels have different lipid compositions. In response, He *et al.*⁷⁶ developed cell membrane chromatography. In cell membrane chromatography, a cell membrane suspension without nuclei is exposed to silica under vacuum and ultrasonication, and the cell membrane adsorbs to the silica.¹⁸⁹ Another alternative is the SM and cholesterol-based IAM column, which has demonstrated predictive performance for BBB permeation similar to that of IAM-PC-DD2 stationary phase.^{189,213}

In the IAM chromatographic procedure, the mobile phase retention factor (k_{IAM}) should be determined

on the IAM stationary phase using a specific equation (Equation [1]):

$$k_{IAM} = \frac{t_R - t_0}{t_0} \quad (1)$$

Where t_R is the retention time of the desired compound or candidate drug, and t_0 is the column void volume.¹⁸⁹ Various buffers and chemicals have been used as aqueous mobile-phase or void-volume markers. However, phosphate-buffered saline is more suitable for physiological conditions.¹⁸⁹

5. Conclusion

In vitro BBB models have been developed and extensively used for evaluating cellular interactions and molecular mechanisms underlying BBB integrity during drug discovery. The main objective of these models is to replicate *in vivo* BBB properties as accurately as possible, including a physiologically realistic cell architecture, a restrictive paracellular pathway, and functional expression of transport mechanisms. Ideally, models should be easily scalable, cost-effective, and conducive to high-throughput screening with reproducible results. However, these models also have limitations. For example, several models have

leaky TJs, making them unsuitable for studying molecule penetration through the paracellular pathway. Therefore, *in vitro* studies should complement *in vivo* studies using the most promising candidate molecules identified during *in vitro* screening.

Recently, generating human BBB cells from iPSCs has emerged as a viable approach for assessing human brain tissue and generating primary cell cultures. Various BBB models reported in the literature focus on developing physiologically relevant models that closely mimic *in vivo* conditions. The incorporation of flow-induced shear stress into BBB models has led to improved barrier function compared to earlier static Transwell models. Recent efforts to integrate cell coculture and biomechanical principles to reflect the complex contributions to neurovascular homeostasis of the NVU and fluid shear stress have made significant advances.

From another perspective, despite the advantages of *in vitro* BBB models for neurological research that facilitate BBB modeling more conveniently and cost-effectively, additional challenges remain. The variability of data or results obtained through different approaches used to validate BBB models depends on experimental conditions across laboratories, which face difficulties with reproducibility and replicability when using *in vitro* BBB models.

In view of that, summarizing various *in vitro* BBB models regarding their conditions and results may provide comprehensive insight and an easier, more inclusive comparison. Beyond this, in recent years, the role of artificial intelligence, machine learning, and deep learning techniques in predicting BBB permeability in drug discovery has been highlighted, as reviewed in other studies.^{214,215} However, Nabi *et al.*²¹⁵ identified several challenges and suggested approaches for developing an ideal predictive model through applying large, diverse, and balanced datasets.

By using machine learning methods and considering multiple features and additional factors, researchers can overcome data variability and improve the accuracy of predictive models. These features may include cell culture media, shear stress levels, NVU cell types (pericytes, astrocytes, neurons, and glial cells), the origin of cells used in cell-based models, and the type of artificial membrane, chromatographic column, or buffer used in cell-free models. They may also represent different conditions, such as normal states or those associated with various neuronal disorders, to facilitate model development.

Moreover, the application of machine learning considering genetic profiles, metabolic signatures, immunophenotyping, and clinical data, such as clinical

positron emission tomography radioligands or *in vivo* brain permeation data, as well as *in vitro* iPSC-based human BBB model data or *in vitro* PAMPA-BBB data,^{209,216} as additional features, could shed light on CNS drug discovery and personalized medicine.

In summary, *in vitro* BBB models, including cell-based and cell-free models, along with their corresponding schematic representations, are outlined in Table 4. Overall, it is essential to continue advancing BBB model simulations to support basic and applied sciences in addressing brain disease problems and studying the cellular mechanisms of brain function. The procedures and considerations discussed in the current review provide a valid starting point for designing experiments and refining existing protocols.

Acknowledgments

We would like to express our gratitude to the Department of Industrial and Environmental Biotechnology at NIGEB.

Funding

Michael J. Strong receives funding from the Canadian Institutes of Health Research (SOP-160442) and the Temerty Family Foundation.

Conflict of interest

The authors declare they have no competing interests.

Author contributions

Conceptualization: Hamdam Hourfar, Farhang Aliakbari, Daniel E. Otzen, Michael J. Strong, Dina Morshedi

Visualization: Arghavan Fattahi

Writing – original draft: Hamdam Hourfar, Arghavan Fattahi, Mohammad Raeji, Kimia Marzookian, Naser Safari, Narges Nasrollahi Boroujeni

Writing – review & editing: Hamdam Hourfar, Farhang Aliakbari, Daniel E. Otzen, Michael J. Strong, Dina Morshedi

Ethics approval and consent to participate

Not applicable.

Consent for publication

Not applicable.

Availability of data

Not applicable.

References

1. Paul SM, Mytelka DS, Dunwiddie CT, *et al.* How to improve R&D productivity: The pharmaceutical industry's grand

- challenge. *Nat Rev Drug Discov.* 2010;9(3):203-214.
doi: 10.1038/nrd3078
2. Ridley H. *The Anatomy of the Brain; Containing its Mechanism and Physiology, Together with some New Discoveries and Corrections of Ancient and Modern Authors upon that Subject. To which is Annex'd a Particular Account of Animal Functions and Muscular Motion.* London: Printed for Sam. Smith and Benj. Walford; 1973.
3. Liddel SA. Fluids and barriers of the CNS: A historical viewpoint. *Fluids Barriers CNS.* 2011;8(1):2.
doi: 10.1186/2045-8118-8-2
4. Ehrlich P. *Das Sauerstoff-Bedürfniss des Organismus: Eine Farbenanalytische Studie.* Berlin: A. Hirschwald; 1885.
5. Barichello T, Collodel A, Hasbun R, Morales R. *Blood-Brain Barrier.* 1st ed. Berlin: Springer; 2019.
doi: 10.1007/978-1-4939-8946-1
6. Goldmann EE. Die äussere und innere skeretion des gesunden Organismus im Lichte der "Vitalen Färbung". [The external and internal skeretion of the healthy organism in the light of the "Vital Colouring"]. *Beiträge zur klinischen Chirurgie: Mittheilungen aus der chirurgischen Klinik zu Tübingen [Contributions to Clinical Surgery: Reports from the Surgical Clinic in Tübingen].* 1909.
7. Reese T, Karnovsky MJ. Fine structural localization of a blood-brain barrier to exogenous peroxidase. *J Cell Biol.* 1967;34(1):207-217.
doi: 10.1083/jcb.34.1.207
8. Banks WA, Erickson MA. The blood-brain barrier and immune function and dysfunction. *Neurobiol Dis.* 2010;37(1):26-32.
doi: 10.1016/j.nbd.2009.07.031
9. Srinivasan B, Kolli AR, Esch MB, Abaci HE, Shuler ML, Hickman JJ. TEER measurement techniques for *in vitro* barrier model systems. *J Lab Autom.* 2015;20:107-126.
doi: 10.1177/2211068214561025
10. Lalatsa A, Butt AM. Physiology of the blood-brain barrier and mechanisms of transport across the BBB. In: *Nanotechnology-Based Targeted Drug Delivery Systems for Brain Tumors.* Amsterdam: Elsevier; 2018. p. 49-74.
doi: 10.1016/B978-0-12-812218-1.00003-8
11. Stamatovic SM, Johnson AM, Keep RF, Andjelkovic AV. Junctional proteins of the blood-brain barrier: New insights into function and dysfunction. *Tissue Barriers.* 2016;4:e1154641.
doi: 10.1080/21688370.2016.1154641
12. Vorbrodt AW, Dobrogowska DH. Molecular anatomy of intercellular junctions in brain endothelial and epithelial barriers: Electron microscopist's view. *Brain Res Rev.* 2003;42:221-242.
doi: 10.1016/s0165-0173(03)00177-2
13. Itoh M, Furuse M, Morita K, Kubota K, Saitou M, Tsukita S. Direct binding of three tight junction-associated MAGUKs, ZO-1, ZO-2, and ZO-3, with the COOH termini of claudins. *J Cell Biol.* 1999;147(6):1351-1363.
doi: 10.1083/jcb.147.6.1351
14. Bhat AA, Uppada S, Achkar IW, *et al.* Tight junction proteins and signaling pathways in cancer and inflammation: A functional crosstalk. *Front Physiol.* 2019;9:1942.
doi: 10.3389/fphys.2018.01942
15. Cording J, Berg J, Käding N, *et al.* In tight junctions, claudins regulate the interactions between occludin, tricellulin and marvelD3, which, inversely, modulate claudin oligomerization. *J Cell Sci.* 2013;126(2):554-564.
doi: 10.1242/jcs.114306
16. Buschmann MM, Shen L, Rajapakse H, *et al.* Occludin OCEL-domain interactions are required for maintenance and regulation of the tight junction barrier to macromolecular flux. *Mol Biol Cell.* 2013;24:3056-3068.
doi: 10.1091/mbc.E12-09-0688
17. Mariano C, Palmela I, Pereira PF, Fernandes A. Tricellulin expression in brain endothelial and neural cells. *Cell Tissue Res.* 2012;351:397-407.
doi: 10.1007/s00441-012-1529-y
18. Abdullahi W, Tripathi D, Ronaldson PT. Blood-brain barrier dysfunction in ischemic stroke: Targeting tight junctions and transporters for vascular protection. *Am J Physiol Cell Physiol.* 2018;315:C343-C356.
doi: 10.1152/ajpcell.00095.2018
19. Jia W, Martin TA, Zhang G, Jiang WG. Junctional adhesion molecules in cerebral endothelial tight junction and brain metastasis. *Anticancer Res.* 2013;33(6):2353-2359.
20. Raleigh DR, Marchiando AM, Zhang Y, *et al.* Tight junction-associated MARVEL proteins MarvelD3, tricellulin, and occludin have distinct but overlapping functions. *Mol Biol Cell.* 2010;21:1200-1213.
doi: 10.1091/mbc.e09-08-0734
21. Steed E, Rodrigues NTL, Balda MS, Matter K. Identification of MarvelD3 as a tight junction-associated transmembrane protein of the occludin family. *BMC Cell Biol.* 2009;10:95.
doi: 10.1186/1471-2121-10-95
22. Crosby CV, Fleming PA, Argraves WS, *et al.* VE-cadherin is not required for the formation of nascent blood vessels but acts to prevent their disassembly. *Blood.* 2005;105:2771-2776.
doi: 10.1182/blood-2004-06-2244
23. Tietz S, Engelhardt B. Brain barriers: Crosstalk between complex tight junctions and adherens junctions. *J Cell Biol.*

- 2015;209:493-506.
doi: 10.1083/jcb.201412147
24. Liebner S, Corada M, Bangsow T, *et al.* Wnt/ β -catenin signaling controls development of the blood-brain barrier. *J Cell Biol.* 2008;183:409-417.
doi: 10.1083/jcb.200806024
25. Takai Y, Irie K, Shimizu K, Sakisaka T, Ikeda W. Nectins and nectins but acts to Roles in cell adhesion, migration, and polarization. *Cancer Sci.* 2003;94:655-667.
doi: 10.1111/j.1349-7006.2003.tb01499.x
26. Kandouz M, Batist G. Gap junctions and connexins as therapeutic targets in cancer. *Expert Opin Ther Targets.* 2010;14:681-692.
doi: 10.1517/14728222.2010.487866
27. Mathias RT, White TW, Gong X. Lens gap junctions in growth, differentiation, and homeostasis. *Physiol Rev.* 2010;90:179-206.
doi: 10.1152/physrev.00034.2009
28. González-Mariscal L, Betanzos A, Ávila-Flores A. MAGUK proteins: Structure and role in the tight junction. *Semin Cell Dev Biol.* 2000;11:315.
doi: 10.1006/scdb.2000.0178
29. Yao Y, Chen ZL, Norris EH, Strickland S. Astrocytic laminin regulates pericyte differentiation and maintains blood brain barrier integrity. *Nat Commun.* 2014;5(1):3413.
doi: 10.1038/ncomms4413
30. Obermeier B, Daneman R, Ransohoff RM. Development, maintenance and disruption of the blood-brain barrier. *Nat Med.* 2013;19(12):1584.
doi: 10.1038/nm.3407
31. Sweeney MD, Zhao Z, Montagne A, Nelson AR, Zlokovic BV. Blood-brain barrier: From physiology to disease and back. *Physiol Rev.* 2019;99(1):21-78.
doi: 10.1152/physrev.00050.2017
32. Mancuso MR, Kuhnert F, Kuo CJ. Developmental angiogenesis of the central nervous system. *Lymphat Res Biol.* 2008;6(3-4):173-180.
doi: 10.1089/lrb.2008.1014
33. Wang Y, Chang H, Rattner A, Nathans J. Frizzled receptors in development and disease. *Curr Top Dev Biol.* 2016;117:113-139.
doi: 10.1016/bs.ctdb.2015.11.028
34. Briscoe J, Thérond PP. The mechanisms of Hedgehog signalling and its roles in development and disease. *Nat Rev Mol Cell Biol.* 2013;14(7):416-429.
doi: 10.1038/nrm3598
35. Gozal E, Jagadapillai R, Cai J, Barnes GN. Potential crosstalk between sonic hedgehog and disease. r. n barrier integrity. the occlusions for blood-brain barrier integrity in autism spectrum disorder. *J Neurochem.* 2021;159(1):15-28.
doi: 10.1111/jnc.15081
36. Xu L, Nirwane A, Yao Y. Basement membrane and blood-brain barrier. *Stroke Vasc Neurol.* 2019;4:78-82.
doi: 10.1136/svn-2018-000198
37. Richter JR, Sanderson RD. The glycocalyx: Pathobiology and repair. *Matrix Biol Plus.* 2023;17:100128.
doi: 10.1016/j.mbpplus.2023.100128
38. Ando Y, Okada H, Takemura G, *et al.* Brain-specific ultrastructure of capillary endothelial glycocalyx and its possible contribution for blood brain barrier. *Sci Rep.* 2018;8(1):17523.
doi: 10.1038/s41598-018-35976-2
39. Kutuzov N, Flyvbjerg H, Lauritzen M. Contributions of the glycocalyx, endothelium, and extravascular compartment to the blood-brain barrier. *Proc Natl Acad Sci U S A.* 2018;115(40):E9429-E9438.
doi: 10.1073/pnas.1802155115
40. Suzuki A, Tomita H, Okada H. Form follows function: The endothelial glycocalyx. *Transl Res.* 2022;247:158-167.
doi: 10.1016/j.trsl.2022.03.014
41. Zhao F, Zhong L, Luo Y. Endothelial glycocalyx as an important factor in composition of blood-brain barrier. *CNS Neurosci Ther.* 2021;27(1):26-35.
doi: 10.1111/cns.13560
42. Du F, Shusta EV, Palecek SP. Extracellular matrix proteins in construction and function of *in vitro* blood-brain barrier models. *Front Chem Eng.* 2023;5:1130127.
doi: 10.3389/fceng.2023.1130127
43. Timpl R, Rohde H, Robey PG, Rennard SI, Foidart JM, Martin GR. Laminin--a glycoprotein from basement membranes. *J Biol Chem.* 1979;254(19):9933-9937.
44. Aumailley M. Chapter 11 - Isolation and analysis of laminins. *Methods Cell Biol.* 2018;143:187-205.
doi: 10.1016/bs.mcb.2017.08.011
45. Yao Y. Basement membrane and stroke. *J Cereb Blood Flow Metab.* 2019;39(1):3-19.
doi: 10.1177/0271678X18801467
46. Gautam J, Zhang X, Yao Y. The role of pericytic laminin in blood brain barrier integrity maintenance. *Sci Rep.* 2016;6:36450.
doi: 10.1038/srep36450
47. Kühn K. Basement membrane (type IV) collagen. *Matrix Biol.* 1995;14(6):439-445.

- doi: 10.1016/0945-053X(95)90001-2
48. Kalluri R. Basement membranes: Structure, assembly and role in tumour angiogenesis. *Nat Rev Cancer*. 2003;3:422.
doi: 10.1038/nrc1094
49. Kangwantis K, Pinteaux E, Penny J. The extracellular matrix protein laminin-10 promotes blood-brain barrier repair after hypoxia and inflammation *in vitro*. *J Neuroinflammation*. 2016;13:25.
doi: 10.1186/s12974-016-0495-9
50. Gautam J, Xu L, Nirwane A, Nguyen B, Yao Y. Loss of mural cell-derived laminin aggravates hemorrhagic brain injury. *J Neuroinflammation*. 2020;17(1):103.
doi: 10.1186/s12974-020-01788-3
51. Halder SK, Kant R, Milner R. Chronic mild hypoxia increases expression of laminins 111 and 411 and the laminin receptor $\alpha 6 \beta 1$ integrin at the blood-brain barrier. *Brain Res*. 2018;1700:78-85.
doi: 10.1016/j.brainres.2018.07.012
52. Jeanne M, Jorgensen J, Gould DB. Molecular and genetic analyses of collagen type IV mutant mouse models of spontaneous intracerebral hemorrhage identify mechanisms for stroke prevention. *Circulation*. 2015;131(18):1555-1565.
doi: 10.1161/CIRCULATIONAHA.114.013395
53. Roberts J, Kahle M, Bix G. Perlecan and the blood-brain barrier: Beneficial proteolysis? Mini review. *Front Pharmacol*. 2012;3:155.
doi: 10.3389/fphar.2012.00155
54. Huang J, Li J, Feng C, *et al*. Blood-brain barrier damage as the starting point of leukoencephalopathy caused by cerebral chronic hypoperfusion and its involved mechanisms: Effect of agrin and aquaporin-4. *Biomed Res Int*. 2018;2018:2321797.
doi: 10.1155/2018/2321797
55. Bader BL, Smyth N, Nedbal S, *et al*. Compound genetic ablation of nidogen 1 and 2 causes basement membrane defects and perinatal lethality in mice. *Mol Cell Biol*. 2005;25(15):6846-6856.
doi: 10.1128/mcb.25.15.6846-6856.2005
56. Kohfeldt E, Sasaki T, Göhring W, Timpl R. Nidogen-2: A new basement membrane protein with diverse binding properties. Edited by I. B. Holland. *J Mol Biol*. 1998;282(1):99-109.
doi: 10.1006/jmbi.1998.2004
57. Iozzo RV. Basement membrane proteoglycans: from cellar to ceiling. *Nat Rev Mol Cell Biol*. 2005;6:646.
doi: 10.1038/nrm1702
58. Bezakova G, Ruegg MA. New insights into the roles of agrin. *Nat Rev Mol Cell Biol*. 2003;4(4):295-309.
doi: 10.1038/nrm1074
59. Rani V, Venkatesan J, Prabhu A. D-limonene-loaded liposomes target malignant glioma cells via the downregulation of angiogenic growth factors. *J Drug Deliv Sci Technol*. 2023;82:104358.
doi: 10.1016/j.jddst.2023.104358
60. Leo A, Hansch C, Elkins D. Partition coefficients and their uses. *Chem Rev*. 1971;71(6):525-616.
doi: 10.1021/cr60274a001
61. Pardridge WM. The blood-brain barrier: Bottleneck in brain drug development. *NeuroRx*. 2005;2(1):3-14.
doi: 10.1602/neurorx.2.1.3
62. Abraham MH, Chadha HS, Mitchell RC. Hydrogen bonding. 33. Factors that influence the distribution of solutes between blood and brain. *J Pharm Sci*. 1994;83(9):1257-1268.
doi: 10.1002/jps.2600830915
63. Gratton JA, Abraham MH, Bradbury MW, Chadha HS. Molecular factors influencing drug transfer across the blood-brain barrier. *J Pharm Pharmacol*. 1997;49(12):1211-1216.
doi: 10.1111/j.2042-7158.1997.tb06072.x
64. Kelder J, Grootenhuys PD, Bayada DM, Delbressine LP, Ploemen JP. Polar molecular surface as a dominating determinant for oral absorption and brain penetration of drugs. *Pharm Res*. 1999;16(10):1514-1519.
doi: 10.1023/a:1015040217741
65. Muehlbacher M, Spitzer GM, Liedl KR, Kornhuber J. Qualitative prediction of blood-brain barrier permeability on a large and refined dataset. *J Comput Aided Mol Des*. 2011;25(12):1095-1106.
doi: 10.1007/s10822-011-9478-1
66. Pajouhesh H, Lenz GR. Medicinal chemical properties of successful central nervous system drugs. *NeuroRx*. 2005;2(4):541-553.
doi: 10.1602/neurorx.2.4.541
67. Cecchelli R, Berezowski V, Lundquist S, *et al*. Modelling of the blood-brain barrier in drug discovery and development. *Nat Rev Drug Discov*. 2007;6:650-661.
doi: 10.1038/nrd2368
68. Warren MS, Zerangue N, Woodford K, *et al*. Comparative gene expression profiles of ABC transporters in brain microvessel endothelial cells and brain in five species including human. *Pharmacol Res*. 2009;59:404-413.
doi: 10.1016/j.phrs.2009.02.007
69. Aliakbari F, Mohammad-Beigi H, Abbasi S, *et al*. Multiple protective roles of nanoliposome-incorporated baicalein against alpha-synuclein aggregates. *Adv Funct Mater*. 2021;31(7):2007765.

- doi: 10.1002/adfm.202007765
70. Parsafar S, Aliakbari F, Seyedfatemi SS, *et al.* Insights into the inhibitory mechanism of skullcapflavone II against α -synuclein aggregation and its mediated cytotoxicity. *Int J Biol Macromol.* 2022;209:426-440.
doi: 10.1016/j.ijbiomac.2022.03.092
 71. Carpenter TS, Kirshner DA, Lau EY, Wong SE, Nilmeier JP, Lightstone FC. A method to predict blood-brain barrier permeability of drug-like compounds using molecular dynamics simulations. *Biophys J.* 2014;107(3):630-641.
doi: 10.1016/j.bpj.2014.06.024
 72. Appelt-Menzel A, Cubukova A, Günther K, *et al.* Establishment of a human blood-brain barrier co-culture model mimicking the neurovascular unit using induced pluri-and multipotent stem cells. *Stem Cell Rep.* 2017;8(4):894-906.
doi: 10.1016/j.stemcr.2017.02.021
 73. Cecchelli R, Dehouck B, Descamps L, *et al.* *In vitro* model for evaluating drug transport across the blood-brain barrier. *Adv Drug Deliv Rev.* 1999;36:165-178.
doi: 10.1016/S0169-409X(98)00083-0
 74. Bhatia SN, Ingber DE. Microfluidic organs-on-chips. *Nat Biotechnol.* 2014;32:760-772.
doi: 10.1038/nbt.2989
 75. Campbell SD, Regina KJ, Kharasch ED. Significance of lipid composition in a blood-brain barrier-mimetic PAMPA assay. *J Biomol Screen.* 2014;19(3):437-444.
doi: 10.1177/1087057113497981
 76. He L, Wang S, Yang G, *et al.* Progress in cell membrane chromatography. *Drug Discov Ther.* 2007;1(2):104-107.
 77. Wilhelm I, Nyúl-Tóth Á, Suciu M, Hermenean A, Krizbai IA. Heterogeneity of the blood-brain barrier. *Tissue Barriers.* 2016;4(1):e1143544.
doi: 10.1080/21688370.2016.1143544
 78. DeStefano JG, Jamieson JJ, Linville RM, Searson PC. Benchmarking in vitro tissue-engineered blood-brain barrier models. *Fluids Barriers CNS.* 2018;15(1):1-15.
doi: 10.1186/s12987-018-0117-2
 79. Wilhelm I, Krizbai IA. *In vitro* models of the blood-brain barrier for the study of drug delivery to the brain. *Mol Pharm.* 2014;11:1949-1963.
doi: 10.1021/mp500046f
 80. Butt AM, Jones HC, Abbott NJ. Electrical resistance across the blood-brain barrier in anaesthetized rats: A developmental study. *J Physiol.* 1990;429:47-62.
doi: 10.1113/jphysiol.1990.sp018243
 81. Hodgkin AL, Katz B. The effect of sodium ions on the electrical activity of the giant axon of the squid. *J Physiol.* 1949;108(1):37.
doi: 10.1113/jphysiol.1949.sp004310
 82. Martin AR. Quantal nature of synaptic transmission. *Physiological reviews.* 1966;46(1):51-66.
doi: 10.1152/PHYSREV.1966.46.1.51
 83. Crone C, Olesen S. Electrical resistance of brain microvascular endothelium. *Brain Res.* 1982;241(1):49-55.
doi: 10.1016/0006-8993(82)91227-6
 84. Erickson MA, Wilson ML, Banks WA. *In vitro* modeling of blood-brain barrier and interface functions in neuroimmune communication. *Fluids Barriers CNS.* 2020;17(1):26.
doi: 10.1186/s12987-020-00187-3
 85. Ahishali B, Kaya M. Evaluation of blood-brain barrier integrity using vascular permeability markers: Evans blue, sodium fluorescein, albumin-alexa fluor conjugates, and horseradish peroxidase. *Methods Mol Biol.* 2021;2367:87-103.
doi: 10.1007/7651_2020_316
 86. Hourfar H, Aliakbari F, Aqdam SR, *et al.* The impact of α -synuclein aggregates on blood-brain barrier integrity in the presence of neurovascular unit cells. *Int J Biol Macromol.* 2023;229:305-320.
doi: 10.1016/j.ijbiomac.2022.12.134
 87. Betz AL, Firth JA, Goldstein GW. Polarity of the blood-brain barrier: Distribution of enzymes between the luminal and antiluminal membranes of brain capillary endothelial cells. *Brain Res.* 1980;192(1):17-28.
doi: 10.1016/0006-8993(80)91004-5
 88. Santaguida S, Janigro D, Hossain M, Oby E, Rapp E, Cucullo L. Side by side comparison between dynamic versus static models of blood-brain barrier *in vitro*: A permeability study. *Brain Res.* 2006;1109(1):1-13.
doi: 10.1016/j.brainres.2006.06.027
 89. Assmann JC, Muller K, Wenzel J, Walther T, Brands J, Thornton P. Isolation and cultivation of primary brain endothelial cells from adult mice. *Bio Protoc.* 2017;7(10):e2294.
doi: 10.21769/BioProtoc.2294
 90. Mizze MR, Miedema SS, van der Poel M, *et al.* Isolation of primary microglia from the human post-mortem brain: Effects of ante-and post-mortem variables. *Acta Neuropathol Commun.* 2017;5(1):16.
doi: 10.1186/s40478-017-0418-8
 91. Aubid NN, Liu Y, Vidal JMP, Hall VJ. Isolation and culture of porcine primary fetal progenitors and neurons from the developing dorsal telencephalon. *J Vet Sci.* 2019;20(2):e3.
doi: 10.4142/jvs.2019.20.e3
 92. Marroni M, Kight KM, Hossain M, Cucullo L, Desai SY,

- Janigro D. Dynamic *in vitro* model of the blood-brain barrier. *Blood Brain Barrier*. 2003;89:419-434.
doi: 10.1385/1-59259-419-0:419
93. Cucullo L, Hossain M, Rapp E, Manders T, Marchi N, Janigro D. Development of a humanized *in vitro* blood-brain barrier model to screen for brain penetration of antiepileptic drugs. *Epilepsia*. 2007;48(3):505-516.
doi: 10.1111/j.1528-1167.2006.00960.x
94. Sano Y, Shimizu F, Abe M, *et al.* Establishment of a new conditionally immortalized human brain microvascular endothelial cell line retaining an *in vivo* blood-brain barrier function. *J Cell Physiol*. 2010;225(2):519-528.
doi: 10.1002/jcp.22232
95. Sivandzade F, Cucullo L. *In-vitro* blood-brain barrier modeling: A review of modern and fast-advancing technologies. *J Cereb Blood Flow Metab*. 2018;38:1667-1681.
doi: 10.1177/0271678X18788769
96. Helms HC, Abbott J, Burek M, *et al.* *In vitro* models of the blood-brain barrier: An overview of commonly used brain endothelial cell culture models and guidelines for their use. *J Cereb Blood Flow Metab*. 2016;36:862-890.
doi: 10.1177/0271678X16630991
97. Eigenmann DE, Xue G, Kim KS, Moses AV, Hamburger M, Oufir M. Comparative study of four immortalized human brain capillary endothelial cell lines, hCMEC/D3, hBMEC, TY10, and BB19, and optimization of culture conditions, for an *in vitro* blood-brain barrier model for drug permeability studies. *Fluids Barriers CNS*. 2013;10:33.
doi: 10.1186/2045-8118-10-33
98. Gomes MJ, Mendes B, Martins S, Sarmiento B. Cell-based *in vitro* models for studying blood-brain barrier (BBB) permeability. In: *Concepts and Models for Drug Permeability Studies*. Amsterdam: Elsevier; 2016. p. 169-188.
doi: 10.1016/B978-0-08-100094-6.00011-0
99. Carter M, Shieh J. Chapter 2-animal behavior. In: *Guide to Research Techniques in Neuroscience*. 2nd ed. San Diego: Academic Press; 2015. p. 39e71.
100. Lippmann ES, Al-Ahmad A, Palecek SP, Shusta EV. Modeling the blood-brain barrier using stem cell sources. *Fluids Barriers CNS*. 2013;10:2.
doi: 10.1186/2045-8118-10-2
101. Cerneckis J, Cai H, Shi Y. Induced pluripotent stem cells (iPSCs): Molecular mechanisms of induction and applications. *Signal Transduct Target Ther*. 2024;9(1):112.
doi: 10.1038/s41392-024-01809-0
102. Moy AB, Kamath A, Ternes S, Kamath J. The challenges to advancing induced pluripotent stem cell-dependent cell replacement therapy. *Med Res Arch*. 2023;11(11):4784.
doi: 10.18103/mra.v11i11.4784
103. Abbott NJ, Dolman DEM, Drndarski S, Fredriksson SM. An improved *in vitro* blood-brain barrier model: Rat brain endothelial cells co-cultured with astrocytes. *Methods Mol Biol*. 2012;814:415-430.
doi: 10.1007/978-1-61779-452-0_28
104. Thomsen LB, Burkhardt A, Moos T. A triple culture model of the blood-brain barrier using porcine brain endothelial cells, astrocytes and pericytes. *PLoS One*. 2015;10:e0134765.
doi: 10.1371/journal.pone.0134765
105. Patabendige A, Skinner RA, Abbott NJ. Establishment of a simplified *in vitro* porcine blood-brain barrier model with high transendothelial electrical resistance. *Brain Res*. 2013;1521:1-15.
doi: 10.1016/j.brainres.2012.06.057
106. Yu F, Kumar NDOS, Foo LC, Ng SH, Hunziker W, Choudhury D. A pump-free tricellular blood-brain barrier on-a-chip model to understand barrier property and evaluate drug response. *Biotechnol Bioeng*. 2020;117(4):1127-1136.
doi: 10.1002/bit.27260
107. Helms HC, Waagepetersen HS, Nielsen CU, Brodin B. Paracellular tightness and claudin-5 expression is increased in the BCEC/astrocyte blood-brain barrier model by increasing media buffer capacity during growth. *AAPS J*. 2010;12:759-770.
doi: 10.1208/s12248-010-9237-6
108. Lippmann ES, Al-Ahmad A, Azarin SM, Palecek SP, Shusta EV. A retinoic acid-enhanced, multicellular human blood-brain barrier model derived from stem cell sources. *Sci Rep*. 2014;4:4160.
doi: 10.1038/srep04160
109. Armulik A, Genové G, Mäe M, *et al.* Pericytes regulate the blood-brain barrier. *Nature*. 2010;468:557-561.
doi: 10.1038/nature09522
110. Menon LG, Shi VJ, Carroll RS. Mesenchymal stromal cells as a drug delivery system. In: *StemBook*. Cambridge: Harvard Stem Cell Institute; 2009.
doi: 10.3824/stembook.1.35.1
111. Liu L, Eckert MA, Riazifar H, Kang DK, Agalliu D, Zhao W. From blood to the brain: Can systemically transplanted mesenchymal stem cells cross the blood-brain barrier? *Stem Cells Int*. 2013;2013:435093.
doi: 10.1155/2013/435093
112. Tian X, Brookes O, Battaglia G. Pericytes from Mesenchymal Stem Cells as a model for the blood-brain barrier. *Sci Rep*. 2017;7(1):39676.
doi: 10.1038/srep39676
113. Furihata T, Kawamatsu S, Ito R, *et al.* Hydrocortisone

- enhances the barrier properties of HBMEC/ciβ, a brain microvascular endothelial cell line, through mesenchymal-to-endothelial transition-like effects. *Fluids Barriers CNS*. 2015;12:7.
doi: 10.1186/s12987-015-0003-0
114. Hoheisel D, Nitz T, Franke H, *et al.* Hydrocortisone reinforces the blood–brain barrier properties in a serum free cell culture system. *Biochem Biophys Res Commun*. 1998;244(1):312–316.
doi: 10.1006/bbrc.1997.8051
115. He Y, Yao Y, Tsirka SE, Cao Y. Cell-culture models of the blood–brain barrier. *Stroke*. 2014;45:2514–2526.
doi: 10.1161/STROKEAHA.114.005427
116. Viña D, Seoane N, Vasquez EC, Campos-Toimil M. cAMP compartmentalization in cerebrovascular endothelial cells: New therapeutic opportunities in Alzheimer's disease. *Cells*. 2021;10(8):1951.
doi: 10.3390/cells10081951
117. Vatine GD, Barrile R, Workman MJ, *et al.* Human iPSC-derived blood-brain barrier chips enable disease modeling and personalized medicine applications. *Cell Stem Cell*. 2019;24:995–1005.e6.
doi: 10.1016/j.stem.2019.05.011
118. Kim J, Chung M, Kim S, Jo DH, Kim JH, Jeon NL. Engineering of a biomimetic pericyte-covered 3D microvascular network. *PLoS One*. 2015;10:e0133880.
doi: 10.1371/journal.pone.0133880
119. Bang S, Na S, Jang JM, Kim J, Jeon NL. Engineering-aligned 3D neural circuit in microfluidic device. *Adv Healthc Mater*. 2016;5:159–166.
doi: 10.1002/adhm.201500397
120. Bang S, Lee SR, Ko J, *et al.* A low permeability microfluidic blood-brain barrier platform with direct contact between perfusable vascular network and astrocytes. *Sci Rep*. 2017;7:8083.
doi: 10.1038/s41598-017-07416-0
121. Marzookian K, Aliakbari F, Hourfar H, Sabouni F, Otzen DE, Morshedi D. The neuroprotective effect of human umbilical cord MSCs-derived secretome against α-synuclein aggregates on the blood-brain barrier. *Int J Biol Macromol*. 2025;304:140387.
doi: 10.1016/j.ijbiomac.2025.140387
122. Aliakbari F, Marzookian K, Parsafar S, *et al.* The impact of hUC MSC-derived exosome-nanoliposome hybrids on α-synuclein fibrillation and neurotoxicity. *Sci Adv*. 2024;10(14):ead13406.
doi: 10.1126/sciadv.adl3406
123. Rohde F, Danz K, Jung N, Wagner S, Windbergs M. Electrospun scaffolds as cell culture substrates for the cultivation of an *in vitro* blood-brain barrier model using human induced pluripotent stem cells. *Pharmaceutics*. 2022;14(6):1308.
doi: 10.3390/pharmaceutics14061308
124. Raeji M, Morshedi D, Mahmoudifard M. Novel simulation of the blood-brain barrier using the polyacrylonitrile electrospun nanofibrous membrane on 3D-printed Transwell. *Polym Adv Technol*. 2024;35(4):e6401.
doi: 10.1002/pat.6401
125. Fazakas C, Wilhelm I, Nagyösi P, *et al.* Transmigration of melanoma cells through the blood-brain barrier: Role of endothelial tight junctions and melanoma-released serine proteases. *PLoS One*. 2011;6:e20758.
doi: 10.1371/journal.pone.0020758
126. Hatherell K, Couraud PO, Romero IA, Weksler B, Pilkington GJ. Development of a three-dimensional, all-human *in vitro* model of the blood–brain barrier using mono-, co-, and tri-cultivation Transwell models. *J Neurosci Methods*. 2011;199:223–229.
doi: 10.1016/j.jneumeth.2011.05.012
127. Cucullo L, Hossain M, Puvenna V, Marchi N, Janigro D. The role of shear stress in Blood-Brain Barrier endothelial physiology. *BMC Neurosci*. 2011;12:40.
doi: 10.1186/1471-2202-12-40
128. Gaillard PJ, de Boer AG. Relationship between permeability status of the blood–brain barrier and *in vitro* permeability coefficient of a drug. *Eur J Pharm Sci*. 2000;12:95–102.
doi: 10.1016/s0928-0987(00)00152-4
129. Gastfriend BD, Palecek SP, Shusta EV. Modeling the blood-brain barrier: Beyond the endothelial cells. *Curr Opin Biomed Eng*. 2018;5:6–12.
doi: 10.1016/j.cobme.2017.11.002
130. Lindroos B, Aho KL, Kuokkanen H, *et al.* Differential gene expression in adipose stem cells cultured in allogeneic human serum versus fetal bovine serum. *Tissue Eng A*. 2010;16:2281–2294.
doi: 10.1089/ten.TEA.2009.0621
131. Hutamekalin P, Farkas AE, Orbók A, *et al.* Effect of nicotine and polyaromatic hydrocarbons on cerebral endothelial cells. *Cell Biol Int*. 2008;32:198–209.
doi: 10.1016/j.cellbi.2007.08.026
132. Smith M, Omid Y, Gumbleton M. Primary porcine brain microvascular endothelial cells: Biochemical and functional characterisation as a model for drug transport and targeting. *J Drug Target*. 2007;15:253–268.
doi: 10.1080/10611860701288539
133. Rice O, Surian A, Chen Y. Modeling the blood-brain barrier

- for treatment of central nervous system (CNS) diseases. *J Tissue Eng.* 2022;13:20417314221095997.
doi: 10.1177/20417314221095997
134. Berezowski V, Landry C, Lundquist S, *et al.* Transport screening of drug cocktails through an *in vitro* blood-brain barrier: Is it a good strategy for increasing the throughput of the discovery pipeline? *Pharm Res.* 2004;21:756-760.
doi: 10.1023/b:pham.0000026424.78528.11
135. Naik P, Cucullo L. *In vitro* blood-brain barrier models: Current and perspective technologies. *J Pharm Sci.* 2012;101:1337-1354.
doi: 10.1002/jps.23022
136. Toyoda K, Tanaka K, Nakagawa S, *et al.* Initial contact of glioblastoma cells with existing normal brain endothelial cells strengthen the barrier function via fibroblast growth factor 2 secretion: A new *in vitro* blood-brain barrier model. *Cell Mol Neurobiol.* 2013;33:489-501.
doi: 10.1007/s10571-013-9913-z
137. Vandenhoute E, Culot M, Gosselet F, *et al.* Brain pericytes from stress-susceptible pigs increase blood-brain barrier permeability *in vitro*. *Fluids Barriers CNS.* 2012;9:11.
doi: 10.1186/2045-8118-9-11
138. Vandenhoute E, Dehouck L, Boucau MC, *et al.* Modelling the neurovascular unit and the blood-brain barrier with the unique function of pericytes. *Curr Neurovasc Res.* 2011;8:258-269.
doi: 10.2174/156720211798121016
139. Nakagawa S, Deli MA, Kawaguchi H, *et al.* A new blood-brain barrier model using primary rat brain endothelial cells, pericytes and astrocytes. *Neurochem Int.* 2009;54:253-263.
doi: 10.1016/j.neuint.2008.12.002
140. Zysk G, Schneider-Wald BK, Hwang JH, *et al.* Pneumolysin is the main inducer of cytotoxicity to brain microvascular endothelial cells caused by *Streptococcus pneumoniae*. *Infect Immun.* 2001;69:845-852.
doi: 10.1128/IAI.69.2.845-852.2001
141. Dehouck MP, M9.2.845-852.2001cer of cytotoxicity to brain microvascular endothelial cells cau-production method to study the blood-brain barrier *in vitro*. *J Neurochem.* 1990;54:1798-1801.
doi: 10.1111/j.1471-4159.1990.tb01236.x
142. Uwamori H, Higuchi T, Arai K, Sudo R. Integration of neurogenesis and angiogenesis models for constructing a neurovascular tissue. *Sci Rep.* 2017;7:17349.
doi: 10.1038/s41598-017-17411-0
143. Koo Y, Hawkins BT, Yun Y. Three-dimensional (3D) tetra-culture brain on chip platform for organophosphate toxicity screening. *Sci Rep.* 2018;8:1-7.
doi: 10.1038/s41598-018-20876-2
144. Alajangi HK, Kaur M, Sharma A, *et al.* Blood-brain barrier: Emerging trends on transport models and new-age strategies for therapeutics intervention against neurological disorders. *Mol Brain.* 2022;15(1):49.
doi: 10.1186/s13041-022-00937-4
145. Engelhardt S, Patkar S, Ogunshola O. Cellw-age strategie-brain barrier regulation in health and disease: A focus on hypoxia. *Br J Pharmacol.* 2014;171(5):1210-1230.
doi: 10.1111/bph.12489
146. Kadry H, Noorani B, Cucullo L. A blood-brain barrier overview on structure, function, impairment, and biomarkers of integrity. *Fluids Barriers CNS.* 2020;17(1):69.
doi: 10.1186/s12987-020-00230-3
147. Yeon JH, Na D, Choi K, Ryu SW, Choi C, Park JK. Reliable permeability assay system in a microfluidic device mimicking cerebral vasculatures. *Biomed Microdevices.* 2012;14:1141-1148.
doi: 10.1007/s10544-012-9680-5
148. Griep LM, Wolbers F, de Wagenaar B, *et al.* BBB ON CHIP: Microfluidic platform to mechanically and biochemically modulate blood-brain barrier function. *Biomed Microdevices.* 2013;15:145-150.
doi: 10.1007/s10544-012-9699-7
149. Booth R, Kim H. Permeability analysis of neuroactive drugs through a dynamic microfluidic *in vitro* blood-brain barrier model. *Ann Biomed Eng.* 2014;42:2379-2391.
doi: 10.1007/s10439-014-1086-5
150. Cho H, Seo JH, Wong KHK, *et al.* Three-dimensional blood-brain barrier model for *in vitro* studies of neurovascular pathology. *Sci Rep.* 2015;5:15222.
doi: 10.1038/srep15222
151. Prabhakarapandian B, Shen MC, Nichols JB, *et al.* Synthetic tumor networks for screening drug delivery systems. *J Controlled Release.* 2015;201:49-55.
doi: 10.1016/j.jconrel.2015.01.018
152. Maoz BM, Herland A, FitzGerald EA, *et al.* A linked organ-on-chip model of the human neurovascular unit reveals the metabolic coupling of endothelial and neuronal cells. *Nat Biotechnol.* 2018;36:865-874.
doi: 10.1038/nbt.4226
153. Xu H, Li Z, Yu Y, *et al.* A dynamic *in vivo*-like organotypic blood-brain barrier model to probe metastatic brain tumors. *Sci Rep.* 2016;6:36670.
doi: 10.1038/srep36670
154. Lim RG, Quan C, Reyes-Ortiz AM, *et al.* Huntington's disease iPSC-derived brain microvascular endothelial cells reveal WNT-mediated angiogenic and blood-brain barrier

- deficits. *Cell Rep.* 2017;19:1365-1377.
doi: 10.1016/j.celrep.2017.04.021
155. Wang YI, Abaci HE, Shuler ML. Microfluidic blood-brain barrier model provides *in vivo*-like barrier properties for drug permeability screening. *Biotechnol Bioeng.* 2017;114:184-194.
doi: 10.1002/bit.26045
156. Zhang W, Gu Y, Hao Y, *et al.* Well plate-based perfusion culture device for tissue and tumor microenvironment replication. *LChip.* 2015;15:2854-2863.
doi: 10.1039/c5lc00341e
157. Huh D, Hamilton GA, Ingber DE. From 3D cell culture to organs-on-chips. *Trends Cell Biol.* 2011;21:745-754.
doi: 10.1016/j.tcb.2011.09.005
158. Bonakdar M, Wasson EM, Lee YW, Davalos RV. Electroporation of brain endothelial cells on chip toward permeabilizing the blood-brain barrier. *Biophys J.* 2016;110:503-513.
doi: 10.1016/j.bpj.2015.11.3517
159. Wong AD, Ye M, Levy AF, Rothstein JD, Bergles DE, Searson PC. The blood-brain barrier: An engineering perspective. *Front Neuroeng.* 2013;6:7.
doi: 10.3389/fneng.2013.00007
160. Hartmann C, Zozulya A, Wegener J, Galla HJ. The impact of glia-derived extracellular matrices on the barrier function of cerebral endothelial cells: An *in vitro* study. *Exp Cell Res.* 2007;313(7):1318-1325.
doi: 10.1016/j.yexcr.2007.01.024
161. Zhang Z, McGoron AJ, Crumpler ET, Li CZ. Co-culture based blood-brain barrier *in vitro* model, a tissue engineering approach using immortalized cell lines for drug transport study. *Appl Biochem Biotechnol.* 2011;163(2):278-295.
doi: 10.1007/s12010-010-9037-6
162. Zobel K, Hansen U, Galla HJ. Blood-brain barrier properties *in vitro* depend on composition and assembly of endogenous extracellular matrices. *Cell Tissue Res.* 2016;365(2):233-245.
doi: 10.1007/s00441-016-2397-7
163. Sisak MAA, Louis F, Matsusaki M. *In vitro* fabrication and application of engineered vascular hydrogels. *Polym J.* 2020;52(8):871-881.
doi: 10.1038/s41428-020-0331-z
164. Kleinman HK, Martin GR. Matrigel: Basement membrane matrix with biological activity. *Semin Cancer Biol.* 2005;15(5):378-386.
doi: 10.1016/j.semcancer.2005.05.004
165. Hughes CS, Postovit LM, Lajoie GA. Matrigel: A complex protein mixture required for optimal growth of cell culture. *Proteomics.* 2010;10(9):1886-1890.
doi: 10.1002/pmic.200900758
166. Benton G, Arnaoutova I, George J, Kleinman HK, Koblinski J. Matrigel: From discovery and ECM mimicry to assays and models for cancer research. *Adv Drug Deliv Rev.* 2014;79-80:3-18.
doi: 10.1016/j.addr.2014.06.005
167. Raia NR, Partlow BP, McGill M, Kimmerling EP, Ghezzi CE, Kaplan DL. Enzymatically crosslinked silk-hyaluronic acid hydrogels. *Biomaterials.* 2017;131:58-67.
doi: 10.1016/j.biomaterials.2017.03.046
168. Partyka PP, Godsey GA, Galie JR, *et al.* Mechanical stress regulates transport in a compliant 3D model of the blood-brain barrier. *Biomaterials.* 2017;115:30-39.
doi: 10.1016/j.biomaterials.2016.11.012
169. Terrell-Hall TB, Ammer AG, Griffith JIG, Lockman PR. Permeability across a novel microfluidic blood-tumor barrier model. *Fluids Barriers CNS.* 2017;14(1):3.
doi: 10.1186/s12987-017-0050-9
170. Potjewyd G, Moxon S, Wang T, Domingos M, Hooper NM. Tissue engineering 3D neurovascular units: A biomaterials and bioprinting perspective. *Trends Biotechnol.* 2018;36(4):457-472.
doi: 10.1016/j.tibtech.2018.01.003
171. Arnaoutova I, George J, Kleinman HK, Benton G. The endothelial cell tube formation assay on basement membrane turns 20: State of the science and the art. *Angiogenesis.* 2009;12(3):267-274.
doi: 10.1007/s10456-009-9146-4
172. Uwamori H, Higuchi T, Arai K, Sudo R. Integration of neurogenesis and angiogenesis models for constructing a neurovascular tissue. *Sci Rep.* 2017;7(1):17349.
173. Antoine EE, Vlachos PP, Rylander MN. Review of collagen I hydrogels for bioengineered tissue microenvironments: Characterization of mechanics, structure, and transport. *Tissue Eng B Rev.* 2014;20(6):683-696.
doi: 10.1089/ten.TEB.2014.0086
174. Kim D, Eom S, Park SM, Hong H, Kim DS. A collagen gel-coated, aligned nanofiber membrane for enhanced endothelial barrier function. *Sci Rep.* 2019;9(1):14915.
doi: 10.1038/s41598-019-51560-8
175. Song L, Yuan X, Jones Z, *et al.* Assembly of human stem cell-derived cortical spheroids and vascular spheroids to model 3-D brain-like tissues. *Sci Rep.* 2019;9(1):5977.
doi: 10.1038/s41598-019-42439-9
176. Van Den Bulcke AI, Bogdanov B, De Rooze N, Schacht EH, Cornelissen M, Berghmans H. Structural and rheological properties of methacrylamide modified gelatin hydrogels.

- Biomacromolecules*. 2000;1(1):31-38.
doi: 10.1021/bm990017d
177. Nichol JW, Koshy ST, Bae H, Hwang CM, Yamanlar S, Khademhosseini A. Cell-laden microengineered gelatin methacrylate hydrogels. *Biomaterials*. 2010;31(21):5536-5544.
doi: 10.1016/j.biomaterials.2010.03.064
 178. Heidari H, Taylor H. Multilayered microcasting of agarose-collagen composites for neurovascular modeling. *Bioprinting*. 2020;17:e00069.
doi: 10.1016/j.bprint.2019.e00069
 179. Barry C, Schmitz MT, Propson NE, *et al*. Uniform neural tissue models produced on synthetic hydrogels using standard culture techniques. *Exp Biol Med*. 2017;242(17):1679-1689.
doi: 10.1177/1535370217715028
 180. Galarza S, Crosby AJ, Pak C, Peyton SR. Control of astrocyte quiescence and activation in a synthetic brain hydrogel. *Adv Healthc Mater*. 2020;9(4):1901419.
doi: 10.1002/adhm.201901419
 181. Ingólfsson HI, Melo MN, Van Eerden FJ, *et al*. Lipid organization of the plasma membrane. *JACS*. 2014;136(41):14554-14559.
doi: 10.1021/ja507832e
 182. Takamura H, Kasai H, Arita H, Kito M. Phospholipid molecular species in human umbilical artery and vein endothelial cells. *J Lipid Res*. 1990;31(4):709-717.
 183. Siakotos A, Rouser G, Fleischer S. Isolation of highly purified human and bovine brain endothelial cells and nuclei and their phospholipid composition. *Lipids*. 1969;4(3):234-239.
doi: 10.1007/BF02532638
 184. Tewes B, Galla HJ. Lipid polarity in brain capillary endothelial cells. *Endothelium*. 2001;8(3):207-220.
doi: 10.1080/10623320109051566
 185. Ribeiro M, Domingues M, Freire J, Santos N, Castanho M. Translocating the blood-brain barrier using electrostatics. *Front Cell Neurosci*. 2012;6:44.
doi: 10.3389/fncel.2012.00044
 186. Mensch J, Jaroskova L, Sanderson W, *et al*. Application of PAMPA-models to predict BBB permeability including efflux ratio, plasma protein binding and physicochemical parameters. *Int J Pharm*. 2010;395(1-2):182-197.
doi: 10.1016/j.ijpharm.2010.05.037
 187. Mensch J, Melis A, Mackie C, Verreck G, Brewster ME, Augustijns P. Evaluation of various PAMPA models to identify the most discriminating method for the prediction of BBB permeability. *Eur J Pharm Biopharm*. 2010;74(3):495-502.
doi: 10.1016/j.ejpb.2010.01.003
 188. Ruell JA, Tsinman KL, Avdeef A. PAMPA-a drug absorption *in vitro* model: 5. Unstirred water layer in iso-pH mapping assays and pKaflux-optimized design (pOD-PAMPA). *Eur J Pharm Sci*. 2003;20(4-5):393-402.
doi: 10.1016/j.ejps.2003.08.006
 189. Tsopeles F, Vallianatou T, Tsantili-Kakoulidou A. Advances in immobilized artificial membrane (IAM) chromatography for novel drug discovery. *Expert Opin Drug Discov*. 2016;11(5):473-488.
doi: 10.1517/17460441.2016.1160886
 190. Kanno K, Wu MK, Scapa EF, Roderick SL, Cohen DE. Structure and function of phosphatidylcholine transfer protein (PC-TP)/StarD2. *Biochim Biophys Acta Mol Cell Biol Lipids*. 2007;1771(6):654-662.
doi: 10.1016/j.bbalip.2007.04.003
 191. Chiu S, Vasudevan S, Jakobsson E, Mashl RJ, Scott HL. Structure of sphingomyelin bilayers: A simulation study. *Biophys J*. 2003;85(6):3624-3635.
doi: 10.1016/S0006-3495(03)74780-8
 192. Ha CE, Bhagavan NV. *Essentials of medical biochemistry: with clinical cases*. Academic Press, 2011.
 193. Maulik P, Shipley G. N-palmitoyl sphingomyelin bilayers: Structure and interactions with cholesterol and dipalmitoylphosphatidylcholine. *Biochemistry*. 1996;35(24):8025-8034.
doi: 10.1021/bi9528356
 194. Li XM, Smaby JM, Momsen MM, Brockman HL, Brown RE. Sphingomyelin interfacial behavior: The impact of changing acyl chain composition. *Biophys J*. 2000;78(4):1921-1931.
doi: 10.1016/S0006-3495(00)76740-3
 195. Kuikka M, Ramstedt B, Ohvo-Rekilä H, Tuuf J, Slotte JP. Membrane properties of D-erythro-N-acyl sphingomyelins and their corresponding dihydro species. *Biophys J*. 2001;80(5):2327-2337.
doi: 10.1016/S0006-3495(01)76203-0
 196. Slotte PJ. Molecular properties of various structurally defined sphingomyelins-correlation of structure with function. *Prog Lipid Res*. 2013;52(2):206-219.
doi: 10.1016/j.plipres.2012.12.001
 197. Zhai X, Boldyrev IA, Mizuno NK, *et al*. Nanoscale packing differences in sphingomyelin and phosphatidylcholine revealed by BODIPY fluorescence in monolayers: Physiological implications. *Langmuir*. 2014;30(11):3154-3164.
doi: 10.1021/la4047098
 198. Galinis-Luciani D, Nguyen L, Yazdani M. Is PAMPA a useful tool for discovery? *J Pharm Sci*. 2007;96(11):2886-2892.
doi: 10.1002/jps.21071

199. Grumetto L, Russo G, Barbato F. Immobilized artificial membrane HPLC derived parameters vs PAMPA-BBB data in estimating *in situ* measured blood–brain barrier permeation of drugs. *Mol Pharm.* 2016;13(8):2808–2816.
doi: 10.1021/acs.molpharmaceut.6b00397
200. Kansy M, Senner F, Gubernator K. Physicochemical high throughput screening: Parallel artificial membrane permeation assay in the description of passive absorption processes. *J Med Chem.* 1998;41(7):1007–1010.
doi: 10.1021/jm970530e
201. Di L, Kerns EH, Fan K, McConnell OJ, Carter GT. High throughput artificial membrane permeability assay for blood–brain barrier. *Eur J Med Chem.* 2003;38(3):223–232.
doi: 10.1016/s0223-5234(03)00012-6
202. Sugano K, Nabuchi Y, Machida M, Aso Y. Prediction of human intestinal permeability using artificial membrane permeability. *Int J Pharm.* 2003;257(1–2):245–251.
doi: 10.1016/s0378-5173(03)00161-3
203. Wohnsland F, Faller B. High-throughput permeability pH profile and high-throughput alkane/water log P with artificial membranes. *J Med Chem.* 2001;44(6):923–930.
doi: 10.1021/jm001020e
204. Huque FT, Box K, Platts JA, Comer J. Permeability through DOPC/dodecane membranes: Measurement and LFER modelling. *Eur J Pharm Sci.* 2004;23(3):223–232.
doi: 10.1016/j.ejps.2004.07.009
205. Dobričić V, Marković B, Nikolic K, Savić V, Vladimirov S, Čudina O. 17 β -carboxamide steroids-*in vitro* prediction of human skin permeability and retention using PAMPA technique. *Eur J Pharm Sci.* 2014;52:95–108.
doi: 10.1016/j.ejps.2013.10.017
206. Fortuna A, Alves G, Soares-Da-Silva P, Falcão A. Optimization of a parallel artificial membrane permeability assay for the fast and simultaneous prediction of human intestinal absorption and plasma protein binding of drug candidates: Application to dibenz [b, f] azepine-5-carboxamide derivatives. *J Pharm Sci.* 2012;101(2):530–540.
doi: 10.1002/jps.22796
207. Jhala D, Chettiar S, Singh J. Optimization and validation of an *in vitro* blood brain barrier permeability assay using artificial lipid membrane. *J Bioequiv Bioavailable.* 2012;14: 1–5.
doi: 10.4172/jbb.S14-009
208. Köllmer M, Mossahebi P, Sacharow E, *et al.* Investigation of the compatibility of the skin PAMPA model with topical formulation and acceptor media additives using different assay setups. *AAPS PharmSciTech.* 2019;20(2):89.
doi: 10.1208/s12249-019-1305-3
209. Kato R, Zeng W, Siramshetty VB, *et al.* Development and validation of PAMPA-BBB QSAR model to predict brain penetration potential of novel drug candidates. *Front Pharmacol.* 2023;14:1291246.
doi: 10.3389/fphar.2023.1291246
210. Barbato F, Cappello B, Miro A, La Rotonda M, Quaglia F. Chromatographic indexes on immobilized artificial membranes for the prediction of transdermal transport of drugs. *Farmaco.* 1998;53(10–11):655–661.
doi: 10.1016/S0014-827X(98)00082-2
211. Pidgeon C, Venkataram U. Immobilized artificial membrane chromatography: Supports composed of membrane lipids. *Anal Biochem.* 1989;176(1):36–47.
doi: 10.1016/0003-2697(89)90269-8
212. Pidgeon C, Marcus C, Alvarez F. Immobilized artificial membrane chromatography: Surface chemistry and applications. In: *Applications of Enzyme Biotechnology.* Berlin: Springer; 1991. p. 201–220.
doi: 10.1007/978-1-4757-9235-5_16
213. De Vrieze M, Verzele D, Szucs R, Sandra P, Lynen F. Evaluation of sphingomyelin, cholesterol, and phosphatidylcholine-based immobilized artificial membrane liquid chromatography to predict drug penetration across the blood-brain barrier. *Anal Bioanal Chem.* 2014;406(25):6179–6188.
doi: 10.1007/s00216-014-8054-7
214. Grant N, Machado Reyes D, Yang Z, Wan L, Wang C, Yan P. Blood brain barrier permeability prediction with artificial intelligence and machine learning: A meta-review and future directions. *Discov Artif Intell.* 2025;5(1):254.
doi: 10.1007/s44163-025-00494-4
215. Nabi AE, Pouladvand P, Liu L, Hua Y, Ayubcha C. Machine learning in drug development for neurological diseases: A review of blood brain barrier permeability prediction models. *Mol Inform.* 2025;44(3):e202400325.
doi: 10.1002/minf.202400325
216. Roux GL, Jarray R, Guyot AC, *et al.* Proof-of-concept study of drug brain permeability between *in vivo* human brain and an *in vitro* iPSCs-human blood-brain barrier model. *Sci Rep.* 2019;9(1):16310.
doi: 10.1038/s41598-019-52213-6